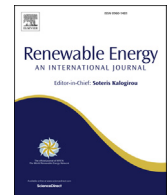




ELSEVIER

Contents lists available at ScienceDirect

# Renewable Energy

journal homepage: [www.elsevier.com/locate/renene](http://www.elsevier.com/locate/renene)

## Long-term extreme response of an offshore turbine: How accurate are contour-based estimates?

Andreas F. Haselsteiner <sup>a,\*</sup>, Malte Frieling <sup>a</sup>, Ed Mackay <sup>b</sup>, Aljoscha Sander <sup>a,c</sup>, Klaus-Dieter Thoben <sup>a</sup>

<sup>a</sup> University of Bremen, BIK – Institute for Integrated Product Development, ForWind – Center for Wind Energy Research, Bremen, Germany

<sup>b</sup> College of Engineering, Mathematics and Physical Sciences, University of Exeter, Penryn, UK

<sup>c</sup> Energy and Sustainability Research Institute Groningen, University of Groningen, Groningen, the Netherlands



### ARTICLE INFO

#### Article history:

Received 24 June 2021

Received in revised form

16 September 2021

Accepted 18 September 2021

Available online 27 September 2021

#### Keywords:

Offshore wind turbine

Environmental contour method

Reliability

Structural design

Multivariate extremes

### ABSTRACT

According to design standards, offshore wind turbines need to withstand environmental loads with a return period of 50 years. This work compares the extreme response along the 50-year environmental contour with the true 50-year wind turbine response. It was found that the environmental contour method that is currently described in the IEC design standard for offshore wind turbines can strongly under-predict the 50-year return value of response variables whose annual maxima typically occur during power production. The bias in the contour-based estimate of the 50-year response can be attributed to three sources: (1) the method used to construct the contour; (2) neglecting serial correlation in environmental conditions; and (3) neglecting the short-term variability in the response. In our analysis the 50-year maximum mudline overturning moment was underestimated by 4–8% by the contour-based approach that is currently recommended, whereas the bending moment at 10 m water depth was underestimated by 25–28%. This underestimation was mainly due to ignoring the short-term variability in the response. The bias associated with contour construction, an effect much discussed in recent publications, was of much smaller magnitude.

© 2021 Elsevier Ltd. All rights reserved.

## 1. Introduction

A major task in the design process of an offshore wind turbine is to evaluate the structural integrity of a candidate design. This evaluation covers fatigue and extreme loads. The widely used international standard IEC 61400-3-1 [1] describes the design process for offshore wind turbines and formulates requirements for structural reliability. Concerning extreme loads, it requires that loads that have a return period of 50 years are assessed by environmental conditions that cause such loads.

To analyze a turbine's response, typically, simulations in the time domain are performed (see, for example [2]). These simulations are computationally expensive and thus it is important to decide which combinations of environmental conditions should be assessed. Some environmental conditions, such as air density or the

type of sea state spectrum, can be kept constant over all simulations, under the assumption that the extreme responses are more sensitive to other environmental variables that exhibit large changes over time, such as wind speed, wave height and wave period. The number of simulations required to cover the full range of combinations of environmental conditions expected over the lifetime of the turbine can be very large. Thus, choosing sensible combinations of environmental variables in which to assess the turbine response is an important part of the design process.

The environmental contour method [3–6] is an approach to define such combinations of environmental variables. The method provides a set of environmental conditions, assumed to cause an extreme response with a given target return period. The method is acknowledged to be a simplified approach, providing an estimate of the true long-term response. Using a full long-term analysis (FLTA) method (see, for example [7–10]) can provide more accurate estimates. However, FLTA methods require the turbine response to be estimated for all combinations of environmental variables, and are therefore not practical for wind turbine design, due to the high computational costs.

\* Corresponding author.

E-mail addresses: [a.haselsteiner@uni-bremen.de](mailto:a.haselsteiner@uni-bremen.de) (A.F. Haselsteiner), [frieling@uni-bremen.de](mailto:frieling@uni-bremen.de) (M. Frieling), [e.mackay@exeter.ac.uk](mailto:e.mackay@exeter.ac.uk) (E. Mackay), [aljoscha.sander@uni-bremen.de](mailto:aljoscha.sander@uni-bremen.de) (A. Sander), [thoben@uni-bremen.de](mailto:thoben@uni-bremen.de) (K.-D. Thoben).

The authoritative design standard IEC 61400-3-1 [1] requires designers to estimate extreme responses using an environmental contour, and does not require the use of FLTA. Researchers, however, have pointed out that applying an environmental contour method to a wind turbine is challenging [11–14]. The turbine's controller actively aims to minimize loading, resulting in non-monotonic responses for many design variables, such as bending moments on the tower and blades. This violates one of the key assumptions underpinning the commonly used inverse first-order reliability method (IFORM) contour approach – that the failure region is convex [4]. Moreover, since the response is sensitive to both wind and wave conditions, reducing the design conditions to a two-dimensional contour of wind speed and wave height introduces further uncertainty, since it neglects the stochastic nature of other variables. Previous studies have proposed modifications to the contour method described in IEC 61400-3-1, mainly based on theoretical arguments. However, as yet it is unclear how contour-based estimates compare to the true long-term response of an offshore wind turbine and how different effects contribute to overall bias of the estimate. Although previous research has tackled this question [11–14], the FLTA methods used in these studies did not account for the serial correlation in environmental data, which causes an overestimation of the response [15]. Further, the research methodology of these studies did not allow to identify the individual sources of bias of a contour-based estimate of the response: Serial correlation, the used definition to construct a contour and a response's short-term variability all contribute to overall bias.

Here, we aim to answer the question: How accurate are contour-based estimates of the long-term response, and how much do different sources of bias contribute to the overall bias of a contour-based estimate of the extreme response? Due to the research methodology applied in this study – applying different types of full long-term analysis based on a 1000-year artificial time series of environmental conditions – we can tackle these questions to gain new insights.

This paper is organized as follows. In section 2 we review the various FLTA methods proposed for estimating the long-term extreme response of an offshore structure. We discuss the environmental contour method and the various approximations that are involved, relative to FLTA. We also review previous studies on the environmental contour method applied to offshore wind turbines. Section 3 describes the study's research methodology and explains how we isolate the various source of bias introduced by the environmental contour approximation. Then, section 4 presents a comparison between the true long-term response and contour-based estimates. Finally, conclusions are presented in section 5.

## 2. Estimating the long-term extreme response

To estimate the long-term extreme response of a structure to environmental loading, three things are required: (1) an environmental dataset; (2) a description of the short-term response as a function of environmental conditions; and (3) a method for combining the short-term response function with the environmental data to estimate the long-term extreme response. There are various methods available for calculating the long-term extreme response. We start by briefly discussing the most accurate types of methods for this task, various methods for 'full long-term analysis' (FLTA). These methods account for the variation of the stochastic short-term response function over the full range of environmental conditions. In subsection 2.1 we consider which type of FLTA method is most appropriate to consider as a reference to compare contour-based estimates to. In subsection 2.2, we discuss environmental contour methods, and the various approximations introduced relative to FLTA methods.

### 2.1. Full long-term analysis methods

The approach taken for FLTA will depend on the return period of interest and the length of environmental data available. If the return period of interest is much less than the length of the environmental dataset, then the short-term response function can be evaluated for each condition in the environmental dataset to obtain a time series of the response, from which the empirical quantile of interest can be obtained. Typically, this requires the environmental dataset to be at least one order of magnitude longer than the return period of interest to keep sampling uncertainties to a reasonable level (see, for example [16]). If the return period of interest is similar or larger than the length of environmental record then we need a way of fitting a model for the long-term distribution to extrapolate outside the range of observations. There are two options for this:

- **Environment-based models:** A probabilistic model of the environmental data is constructed and used to extrapolate outside the range of observations. The extrapolated environmental conditions are then combined with the short-term response function to estimate the long-term extreme response.
- **Response-based models:** The environmental data is combined with the response function to obtain a time series of response. A probabilistic model is fitted to the response data and used to extrapolate to the return period of interest.

The advantage of response-based methods is that the problem of predicting long-term extremes is reduced to a univariate problem. However, the disadvantage is that a separate probabilistic analysis needs to be conducted for each response of interest. Moreover, response-based methods make the tacit assumption that the behavior of the response function does not change significantly outside the range of observations. As discussed further below, this assumption may not be appropriate for a wind turbine response, such as tower or blade bending moments. For example, at some locations, the largest responses in short environmental records may occur in operational conditions, whereas for longer return periods the largest responses may occur when the turbine is parked or idling. As the form of the response function can differ in operational and parked conditions, extrapolating based on observed responses over a short time period may lead to errors.

Environment-based extrapolation can be more complex to implement, since it typically involves a multivariate problem, such as fitting a model for the joint distribution of wind and wave conditions. However, it has the advantage that a single extreme value analysis of environmental conditions can be conducted and used to estimate multiple extreme responses. Moreover, no assumptions are required about how the response function behaves outside the range of observations, since the response function is evaluated explicitly for the extreme environmental conditions.

Another key distinction between FLTA methods is the treatment of serial correlation. Table 1 presents some examples of FLTA methods using environment-based and response-based extrapolation, categorized by whether they assume (a) individual response peaks ("all-peaks"); (b) short-term maxima; or (c) storm-peak values are independent. Here, 'short-term maxima' refers to the maxima in each record of the environmental dataset, typically over time-scales of 100 minutes – 3 hours, whereas "all-peaks" methods consider all response peaks within each record as independent (typically there will be several hundred response cycles per hour). The correlation time-scales in the short-term response function are typically much shorter than the time-scales of the environmental records. This means that if the environmental conditions were

**Table 1**  
Examples of full long-term analysis methods used for estimating extreme responses.

Events considered independent	Environment-based models	Response-based models
All response peaks	Nordenström [22] Battjes [23] Tucker [24] Guedes Soares [25] Naess [26]	
Short-term maxima	Krogstad [27] Videiro and Moan [7] Moriarty et al. [28] Fogle et al. [8] Sagribo et al. [9] Muliawan et al. [29] Videiro et al. [30] Gramstad et al. [31] Brown et al. [37] Hansen et al. [38] Mackay and Jonathan [39]	Marshall et al. [32] Standing et al. [33] Mazaheri and Downie [34] Fontaine et al. [35] Vanem et al. [36]
Storm-peak values		Tromans and Vanderschuren [40] Bowers et al. [41] Inceci et al. [42] Mackay and Johanning [43,44] Koochi Kheili et al. [45]

stationary, then it would be reasonable to assume that extreme responses separated by, for example, 1 hour, are independent. However, since the size of the response depends on the environmental condition, and time series of environmental conditions are serially correlated, time series of extreme responses will also exhibit serial correlation. Table 1 also includes some examples of methods for estimating long-term extremes of individual wave or crest heights, since these can be considered as FLTA methods, where the response function is the short-term wave or crest height distribution. The list of works cited in Table 1 is far from exhaustive, and there is a large volume of literature on this topic. The purpose of the table is to illustrate the types of methods proposed and the key assumptions made.

Comparisons between all-peaks, short-term maxima and storm-peak methods have been presented in Refs. [9,15,17,18]. All-peaks and short-term maxima methods neglect the serial correlation in environmental conditions. Mackay et al. [15] showed that this can lead to significant positive biases in estimates of long-term extreme responses, with the bias being larger when the distribution of storm-peak values has a longer tail. Nevertheless, environment-based short-term maxima FLTA methods are widely used in ocean engineering and as reference methods for estimating extreme loads on offshore wind turbines [11–14]. Moreover, they are the basis for the first- and second-order reliability methods (FORM and SORM) [19] and inverse FORM and SORM methods [20,21].

Based on the discussion above, storm-based methods with environment-based extrapolation are considered most accurate for estimating the long-term extreme response of an offshore wind turbine. This method will therefore be used as the reference method in this study.

## 2.2. Environmental contours for wind turbine design

Compared to storm-based FLTA methods, the environmental contour method introduces three simplifying assumptions:

1. The maximum responses in each short-term condition are independent
2. The  $N$ -year response occurs at an  $N$ -year environmental extreme
3. The response in each environmental condition can be evaluated at a fixed quantile of the short-term distribution function

As discussed in the previous section, the first simplification is also applied in some commonly used FLTA methods. The second simplification is related to the assumption about the failure surface,

made in the construction of the contour. IFORM contours [4] (and various alternative formulations [46,47], which we also refer to here as IFORM methods) are based on the assumption that a structure's failure surface can be linearized at the design point (the point on the failure surface with the highest probability of occurrence). Under this assumption, multivariate extreme sets are defined as half-plane regions, corresponding to the linearized failure surface, which contain a fixed probability level  $\alpha$ . The environmental contour is then defined as the boundary of the region consisting of the intersection of all such extreme sets. The alternative assumption is to assume that structural failure occurs anywhere outside the design region (see, for example [48,49]). Under this assumption, an environmental contour is defined as the boundary to a region containing probability  $1 - \alpha$ . Differences between these two types of contour are discussed in Ref. [6].

The third simplification is equivalent to assuming the short-term response function is deterministic rather than random, with the deterministic response defined as the response at the fixed quantile of the short-term distribution function. As the response of the structure is only evaluated in environmental conditions along the contour, this neglects the probability that the 50-year response could be caused by a high response in less extreme environmental conditions or a low response in a more extreme condition. The effect of short-term variability is usually accounted for by evaluating the short-term response at a quantile higher than the median value [4].

In addition to the three simplifying assumptions listed above, the accuracy of the environmental contour method is dependent on three additional factors:

4. The reduction of a high-dimensional multivariate problem to a 2D or 3D problem
5. The accuracy of the joint probability model for the environmental variables
6. The accuracy of the response model

These factors also influence the accuracy of FLTA methods. The response of many offshore structures are dependent on multiple environmental variables (see the discussion in subsection 3.1). However, due to the difficulty in estimating joint distributions in high dimensions and the number of simulations required to characterize the response in a high dimensional space, it is normally assumed that certain variables are either fixed or in fixed relation to other variables, so that only two or three variables need to be considered.

The environmental contour method is used to establish design loads for offshore wind turbines (see, for example, [11–14,50–53]; Table 2). In design load case (DLC) 1.6 in IEC 61400-3-1 [1], it is required that the design is checked for combinations of wind speed and significant wave height along a 50-year environmental contour (Fig. 1). Compared to other marine structures, applying a contour method to offshore wind turbine design presents particular challenges. The environmental contour method was mainly developed for structures for which the wave height and period have the dominant influence on the response. For an offshore wind turbine both wind and wave loads are equally important. Thus, the effect of reducing the wind turbine design problem to a 2D contour may have a greater impact than for other structures.

The IEC standard recommends to use IFORM contours for DLC 1.6. As discussed above, the IFORM approach assumes that a structure's failure surface can be linearized at the design point. While the linearization is reasonable for many marine structures, it is problematic for many wind turbine response variables. Modern wind turbines have control systems that optimize power output while reducing loads. The controller is designed to extract as much power as possible from the wind until the power output reaches the rated capacity, at the rated wind speed, which is typically around 11–13 m s<sup>-1</sup>. Above this wind speed, the blades are progressively pitched to reduce loads while maintaining constant power output. Finally, at the cut-out wind speed, turbines stop producing power and the blades are fully pitched out of the wind to minimize loads. Consequently, some response variables such as the mudline overturning moment do not increase monotonically with wind speed (see Fig. 2; [12,51,54]).

Thus, researchers have pointed out that such an IFORM contour should not be applied directly in offshore wind turbine design (see, for example [12–14]). Essentially, the non-monotonic response over wind speed leads to two distinct regions of high response along the environmental contour such that the failure surface cannot be well approximated by linearizing it at a single point (Fig. 2). As a solution, Li et al. [12] proposed to use a procedure that involves checking multiple environmental contours with different return periods. Horn and Winterstein [13] also acknowledged the problem and proposed to divide the wind-wave variable space, with the turbine in power production and parked mode, into four

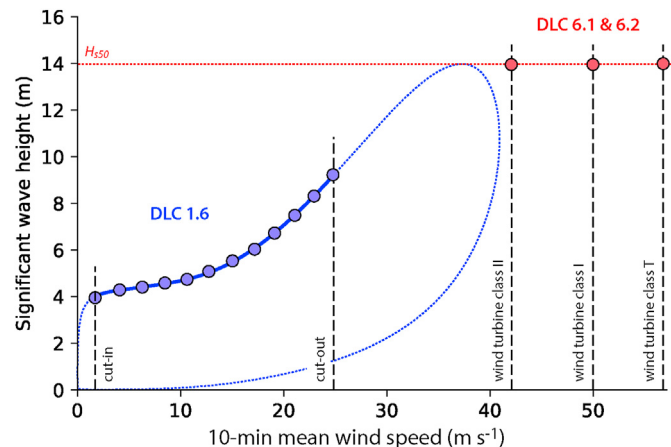


**Fig. 1.** Design approach in IEC 61400-3-1 [1]. In design load case (DLC) 1.6, loads are evaluated at points along a 50-year wind-wave environmental contour, for wind speeds between cut-in and cut-out. At higher wind speeds, DLCs 6.1 and 6.2 require that the 50-year marginal significant wave height value,  $H_{s50}$ , and the reference wind speed value are combined. Reference wind speeds are based on the turbine classes defined in IEC 61400-1 [55] and must be higher than a site's 50-year wind speed. Circles show environmental conditions that must be considered based on the three load cases. Note that  $H_{s50}$  does not necessarily coincide with the highest point along the contour in a 50-year IFORM contour, but that it depends on the order of the variable transformation [6].

sub-populations and to construct one contour per sub-population. Velarde et al. [14] focused on the sea state's frequency variation and proposed an environmental contour method to assess the wave peak period that causes the highest response.

The factors that are relevant for all marine structures have already been analyzed to a great extent in the literature. The uncertainty of choosing a joint model has been analyzed in a recent benchmarking study on environmental contours [56,57]. Different definitions for contour exceedance have been analyzed [6,58–60]. Short-term variability has been discussed in an early paper by Winterstein et al. [4] and since then analyzed for various structures [29,61]. Practical methods for accounting for short-term variability in contour methods are discussed in Refs. [62,63]. The effect of

**Table 2**

Environmental contour methods proposed for analyzing offshore wind turbine reliability.  $V$  = wind speed,  $TI$  = turbulence intensity,  $H_s$  = significant wave height,  $T_p$  = spectral peak period.

Source and year	Contour variables	Additional deterministic variable	Contour type	Analyzed here
Saranyasontorn and Manuel [11], 2006	$V, H_s$	—	50-year IFORM	—
Li et al. [12,51], 2016, 2017	$V, H_s, T_p$	—	Modified IFORM that restricts the contour to wind speeds $< 25 \text{ m s}^{-1}$	—
Horn and Winterstein [13] 2018	$V - H_s \& H_s - T_p$	$T_p$ and $V$ , respectively	Four 50-year IFORM contours, one per variable space sub-population	—
Velarde et al. [14] 2019	$H_s, T_p$	$V$	Multiple $N$ -year IFORM contours, value of $N$ determined based on $V$	—
Liu et al. [52] 2019	$V, H_s$	$T_p$ , median $T_p V, H_s$ is used	50-year IFORM	X
IEC 61400-3-1, DLC 1.6 [55] 2019	$V, H_s$	$T_p$ , highest load $T_p V, H_s$ is used <sup>a</sup>	50-year IFORM	X
Chen et al. [53] 2020	$V, TI, H_s, T_p$	—	50-year IFORM and modified IFORM	—
This work	$V, H_s$	$T_p$ , median $T_p V, H_s$ is used	50-year highest density	X
This work	$V, H_s$	$T_p$ , highest load $T_p V, H_s$ is used	50-year highest density	X
This work	$V, H_s, T_p$	—	50-year highest density	X

<sup>a</sup> Guidance on choosing values is not definitive. The standard's text reads "The severe sea state shall include the extreme individual wave height that, in combination with the associated wave period and the mean wind speed, has a return period of 50 years. The designer shall take account of the range of wave period,  $T$ , appropriate to each extreme wave height. In the absence of a more sophisticated probabilistic assessment, design calculations shall assume values of wave periods within this range that results in the highest loads acting on an offshore wind turbine."

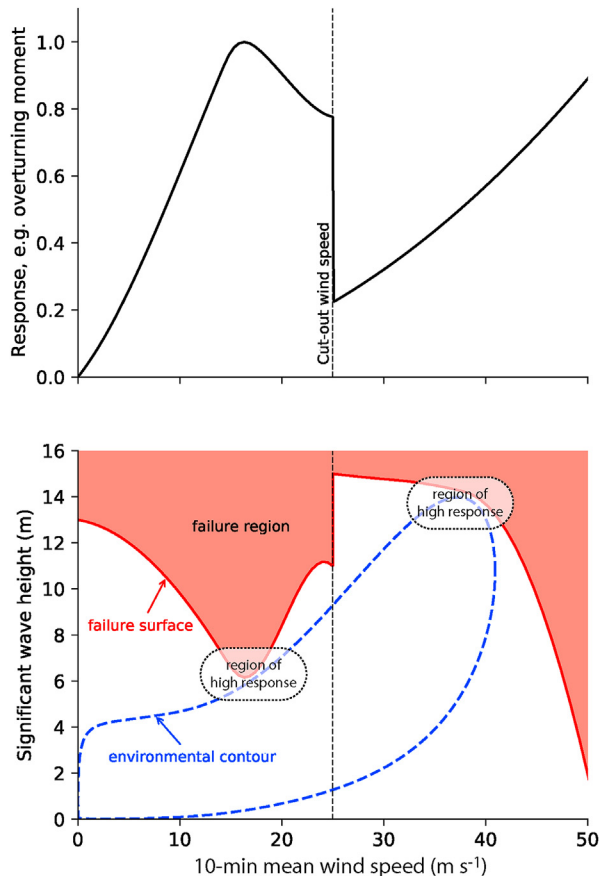


**Fig. 2.** Non-monotonic response of an offshore wind turbine (top) and the associated problem when an environmental contour is used for structural design (bottom). Top: Due to a turbine's control system, response variables such as the overturning moment or the fore-aft shear force are non-monotonic (see, for example [12,51,54]). Bottom: As a consequence, the failure region is non-convex and the contour has two regions of high response. This can be problematic for IFORM contours, which approximate failure surfaces as hyperplanes, which is only conservative if the failure region is convex.

serial correlation on environmental contours and estimates of long-term extreme loads has been discussed in Refs. [15,47]. The two challenges associated with offshore wind turbines, dealing with the non-monotonic response and jointly dealing with wind and wave variables, are less understood.

The problem of the non-monotonic response violating the assumptions of IFORM contours can be addressed by using a contour that is defined based on the total exceedance probability outside the contour. For such contours a non-monotonic response does not violate any assumptions [6,48,49]. Non-monotonic responses are problematic for IFORM contours because they can lead to non-convex failure regions and IFORM is only conservative for convex failures regions. Total exceedance contours, such as highest density contours [48] and Chai and Leira's inverse second-order reliability method (ISORM; [49]) contours yield always conservative environmental design conditions (provided that short-term variability is accounted for).

For addressing the relevant variables – wind speed, wave height, wave period and potentially turbulence intensity (see Ref. [53]) – in a contour method, there is no clear solution in the literature. The design standard IEC 61400-3-1 [1] suggests that a 2D wind speed - wave height contour should be constructed and that spectral peak period should be chosen as the period that causes the highest loads at the particular combination of wind speed and wave height. While this approach sounds somewhat sensible, this

combination of probabilistic and deterministic choices of variables cannot be interpreted consistently in terms of failure probability and implied reliability. Velarde et al. [14], however, proposed that the joint distribution of wind speed, significant wave height ( $H_s$ ) and spectral peak period ( $T_p$ ) shall be used to construct multiple  $H_s - T_p$  contours instead. Horn and Winterstein [13] proposed to use multiple 2D contours, both wind speed - wave height and wave height - wave period to deal with the three-dimensional variable space. In principle, environmental contour methods generalize to higher dimensions [4,48,64] such that one could also construct a single three-dimensional wind speed, wave height, wave period surface, (which we also refer to as a “contour”, for consistency). Currently, it is unclear which of these approaches is best suited to deal with the environmental variables that are relevant to offshore wind turbine design.

Past works have analyzed the design loads on wind turbines using various contour methods [11,12,14,51–53] and have proposed new contour methods based on theoretical arguments. Where the environmental contour method for wind turbines has been compared to FLTA, the FLTA method applied has been based on the assumption that hourly environmental extremes are independent. As discussed in Ref. [15], hourly observations are strongly serially correlated and neglecting serial correlation can result in positive biases in estimates of long-term extreme response. Thus, as yet, no study has compared response estimates from contours with the true unbiased long-term response of an offshore wind turbine. This study aims to provide such a comparison.

### 3. Research methodology

This study's overall design is summarized in Fig. 3. The goal is to compare the “true” 50-year long-term response with an estimate based on an environmental contour. Of the factors affecting the accuracy of the long-term response estimates, discussed in subsection 2.2, we do not consider the accuracy of the response model or the accuracy of the statistical model for environmental

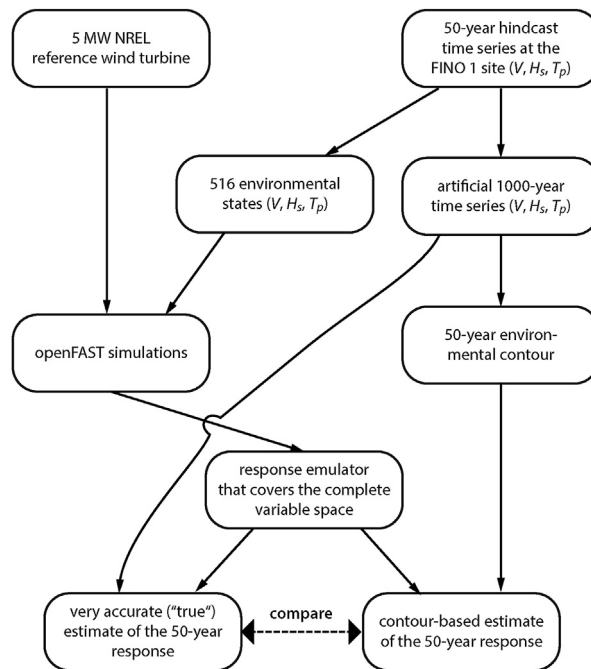


**Fig. 3.** Research methodology. This study's goal is to compare the “true” long-term response with an estimate based on an environmental contour. To enable this comparison a response emulator and an artificial 1000-year time series of environmental conditions are created.

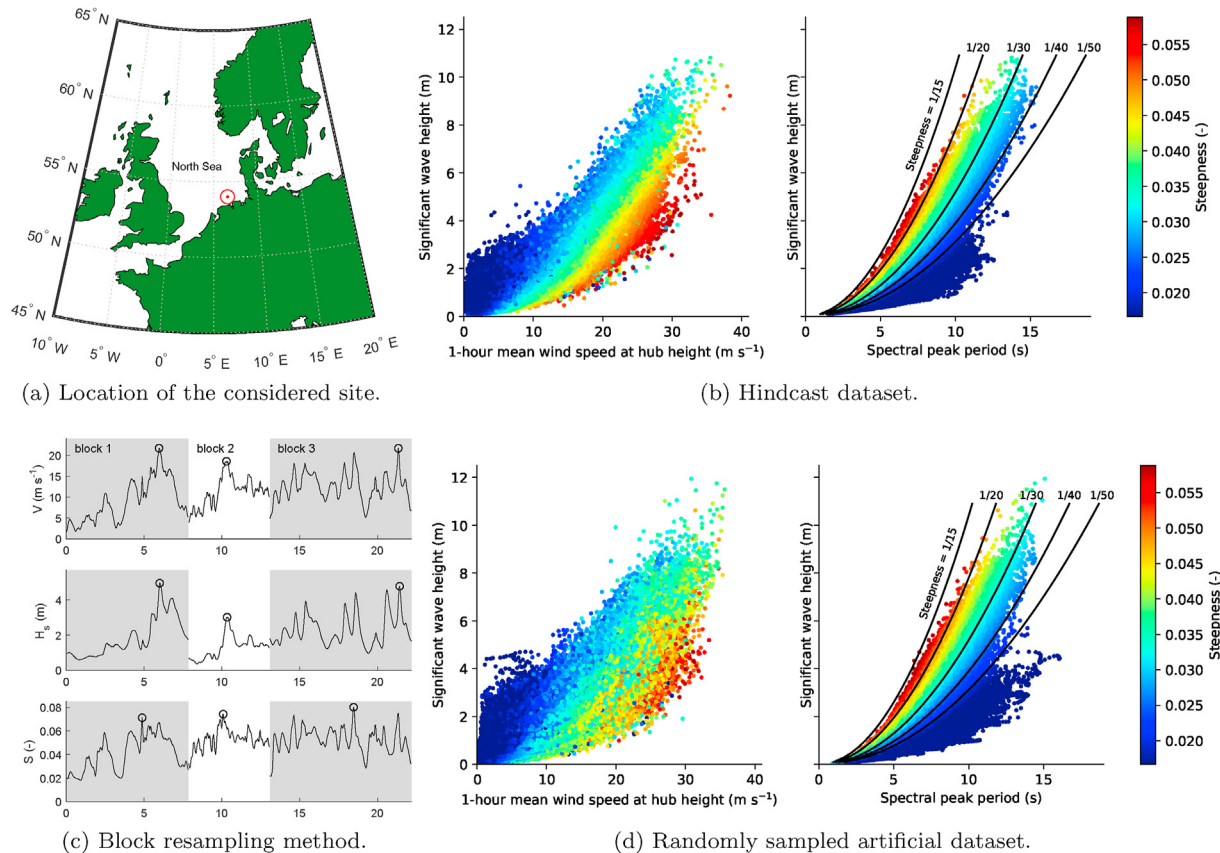


**Fig. 4.** Metocean dataset. (a–b) A 50-year period of the coastDat-2 dataset [67] at the location of the FINO 1 research platform was used to build a statistical model. The three variables considered were 1-hour mean wind speed at hub height, 1-hour significant wave height and 1-hour spectral peak period. (c–d) An artificial dataset was created that spans 1000 years (the first 50 years are shown here), with statistical characteristics matching the coastDat-2 dataset. The dataset was created using a block-resampling method, where block-peak values (shown as circles) were drawn randomly from a joint model and measured blocks are resampled and rescaled so that the peak values match the simulated values.

conditions, since these factors influence both contour and FLTA methods. Instead, we focus on isolating the influence of the approximations made in the environmental contour method relative to FLTA.

We use the 5 MW NREL reference wind turbine [65] and consider the FINO 1 research platform site in the German North Sea [66]. Because performing dynamic multiphysics simulations of a wind turbine with a state-of-the-art code such as openFAST requires CPU computation time in the same or a higher order of magnitude as the simulation time, simulating times series that cover multiple years is impractical. Thus, we created a response emulator based on 516 1-hour multiphysics simulations. This response emulator is a parametric statistical model that outputs a random 1-hour maximum response for a given environmental condition. Additionally, to estimate the 50-year response accurately, a much longer time series than measurements or hindcasts offer is required. Consequently, we created an artificial 1000-year time series. This time series and the response emulator were used to accurately estimate the 50-year response. Finally, we also used the response emulator and the empirical joint distribution derived from the artificial time series to calculate contour-based estimates of the 50-year response. The methodology is described in detail in the following subsections.

### 3.1. Environmental conditions

To enable a comparison between a very accurate estimate, (which we refer to as the “true” long-term response), and estimates

from contour methods, we needed to consider a time series that is several orders of magnitude longer than the return period of interest. Typical site-specific datasets of wind speed and wave height, however, only cover periods of the order of 10–100 years. To circumvent this problem, here, we generated an artificial time series, based on the statistical characteristics of a 50-year dataset from the coastDat-2 hindcast [67,68] at the location of the FINO 1 research platform in the German North Sea (Fig. 4). This 50-year dataset was also used in a recent benchmarking exercise on environmental contours [56].

The artificial time series was created using a block resampling method [39]. The method involves three steps. In the first step, the time series is divided into non-overlapping blocks, where the peaks of each variable of each block can be considered approximately independent from adjacent blocks (in a similar manner to a peaks-over-threshold analysis). In the second step, a joint distribution model is fitted to the block-peak values. In the third step, random vectors of peak values are simulated from the fitted model and measured blocks with peak values closely-matching the simulated values are selected at random and rescaled so that the resampled and simulated peak values coincide. The artificial time series is composed of the resampled and rescaled blocks from the original time series. The idea is that, provided that the measured blocks are only scaled by a small amount, the resampled time series should be physically realistic and closely match both the temporal and joint dependence structure of the measured time series. The resampled time series is not continuous at the block boundaries. However, the blocks are defined so that the peak values do not occur near the

block boundaries, so that the temporal correlation structure around the peak values is preserved. Further details of the procedure used to generate the artificial time series are presented in the [supplemental material](#).

The artificial time series covers 1000 years. Although the focus of the present work is to estimate 50-year responses, a much longer time series is required so that sampling uncertainties are reduced. For example, in a given 50-year time series, the sampling uncertainty in the largest value is extremely high. It can be shown that a  $1 - 2\alpha$  confidence interval (CI) for the return period associated with the largest observation in an  $N$ -year time series tends to  $(-N/\log(\alpha), -N/\log(1-\alpha))$  as  $N \rightarrow \infty$  [16]. So a 95% CI for the return period of the largest response in a 50-year time series would be (13.6, 1975) years. The width of the CI decreases as the ratio of  $N/T$  increases, where  $N$  is the length of the time series and  $T$  is the target return period (see Ref. [16] for a discussion of this). A 95% CI for the return period associated with the 50-year response estimated from a 1000-year time series is (33.9, 81.6) years (CIs for the estimated responses are shown in Fig. 4).

The environmental model comprised a joint distribution for block maxima of wind speed,  $V$ , significant wave height,  $H_s$ , and wave steepness,  $S = 2\pi H_s/gT_p^2$  (where  $g$  is the acceleration due to gravity). Comparisons of measured and simulated values of these variables are shown in Fig. 4.

In the present work, we have only considered the variation of wind speed, significant wave height and wave steepness. The environmental variables that were assumed to remain constant over time are listed in Table 3.

### 3.2. Wind turbine response

#### 3.2.1. Turbine properties

We used the 5 MW NREL reference wind turbine [65] with the monopile design that was proposed by Bachynski et al. [69]. Fig. 5 shows the turbine's main dimensions, the three variables that were varied among simulations – wind speed, significant wave height and spectral peak period – and the response variables that were analyzed, the bending moment at 10 m water depth and the mudline overturning moment. The turbine is controlled via a variable-speed-variable-pitch scheme, with a cut-in wind speed of 3 m s<sup>-1</sup> and a cut-out wind speed of 25 m s<sup>-1</sup>.

#### 3.2.2. Multiphysics simulations

We performed aero-hydro-servo-elastic simulations using the code openFAST ([70], version 2.2.0). OpenFAST is a multiphysics simulation code that allows the coupled simulation of aerodynamics ("aero"), hydrodynamics ("hydro"), structural dynamics ("elasto") and a controller ("servo"). The code consists of several software modules that deal with different types of physics. The software module AeroDyn [71] handles the aerodynamics and is based on the principle of actuator lines. We used its

implementation of the blade element momentum method. The software module HydroDyn handles the hydrodynamics. We used its implementation of strip theory that is based on Morison's equation and linear wave theory to simulate wave loads. Structural mechanics were handled by the modules ElastoDyn (rotor blades, tower and transition piece) and SubDyn ([72]; monopile).

Simulations were run for a total duration of 1 hour and 30 s, however, the first 30 s were discarded because they were only intended to initialize the simulation to a dynamic state. The time step size was 12.5 ms. We performed simulations which covered the range of observed wind speeds, wave heights and wave periods (Fig. 6). Thus, simulations were performed for wind speeds between 1 and 45 m s<sup>-1</sup>, significant wave heights between 0 and 15 m and spectral peak periods between ca. 3 s and 18 s. The variable space was evaluated by performing simulations at four different  $T_p$  values per  $V - H_s$  combination. These four "slices" of  $T_p$  through the 3-dimensional variable space were defined as:

$$\begin{aligned} t_{p1} &= \sqrt{\frac{2\pi h_s}{g \cdot 0.066}}, & t_{p2} &= \sqrt{\frac{2\pi h_s}{g \cdot 0.04}}, & t_{p3} &= t_{p2} + \frac{8}{1 + \sqrt{h_s + 2}}, \\ t_{p4} &= t_{p2} + \frac{20}{1 + \sqrt{h_s + 2}}, \end{aligned} \quad (1)$$

where  $g = 9.81$  m s<sup>-2</sup> is the acceleration due to gravity. In total 516 simulations were performed to cover the variable space.

#### 3.2.3. Statistical response emulator

We built a response emulator that returns a random 1-hour maximum moment at 30 m water depth for a given combination of 1-hour mean wind speed  $v$ , significant wave height  $h_s$  and peak period  $t_p$ . In principle, such a response emulator can be defined in various ways. Here, we chose to define the emulator as a parametric distribution of the short-term response maxima such that a random 1-hour maximum can be drawn by calling the distribution's inverse cumulative distribution function. Let  $F_{1h}(r|v, h_s, t_p)$  denote the conditional distribution function of the 1-hour maximum mudline overturning moment. Thus the 1-hour maximum overturning moment is a random variable  $R$  and its realization is denoted  $r$ . Then the response emulator is the inverse distribution function:

$$F_{1h}^{-1}(p|v, h_s, t_p), \quad (2)$$

which can be called with a value for  $p \in [0, 1]$  to evaluate a given quantile of interest. To draw a random 1-hour response realization, we simulated uniformly distributed random variables  $p \in [0, 1]$  and then calculated  $F_{1h}^{-1}(p|v, h_s, t_p)$ .

The distribution of short-term response maxima can be estimated using various techniques, such as block-maxima, peaks-over-threshold, or up-crossing rate methods [73–76]. Here, we

**Table 3**

Environmental variables that are constant over all simulations.

Air density	1.225 kg m <sup>-3</sup>
Wind speed profile	$V(z) = V_{hub}(z/z_{hub})^{0.14}$
Turbulence intensity	During power production: ca. 14%–50% (wind turbine class B; IEC 61400-1 normal turbulence model) Above 25 m s <sup>-1</sup> : 11% (IEC 61400-1 normal turbulence model)
Water density	1025 kg m <sup>-3</sup>
Wave spectrum	JONSWAP spectrum with $\gamma = 3.3$
Wave directional spread	0 deg
Wave mean direction	0 deg
Wind mean direction	0 deg
Current velocity	0 m s <sup>-1</sup>
Water depth	30 m

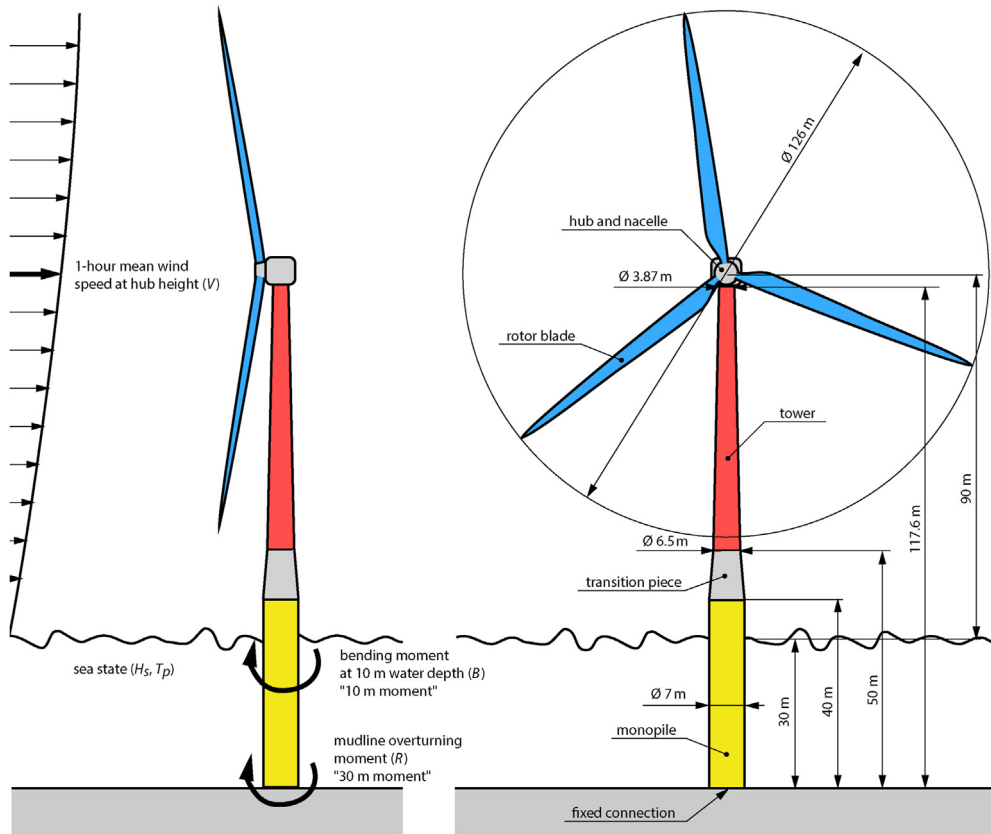


**Fig. 5.** 5 MW NREL reference wind turbine [65] with the monopile foundation presented by Bachynski et al. [69]. In this study, we varied the three environmental conditions 1-hour mean wind speed ( $V$ ), significant wave height ( $H_s$ ) and spectral peak period ( $T_p$ ). For simplicity, only two response variables, the mudline overturning moment ( $R$ ) and the bending moment at 10 m water depth ( $B$ ), were analyzed.

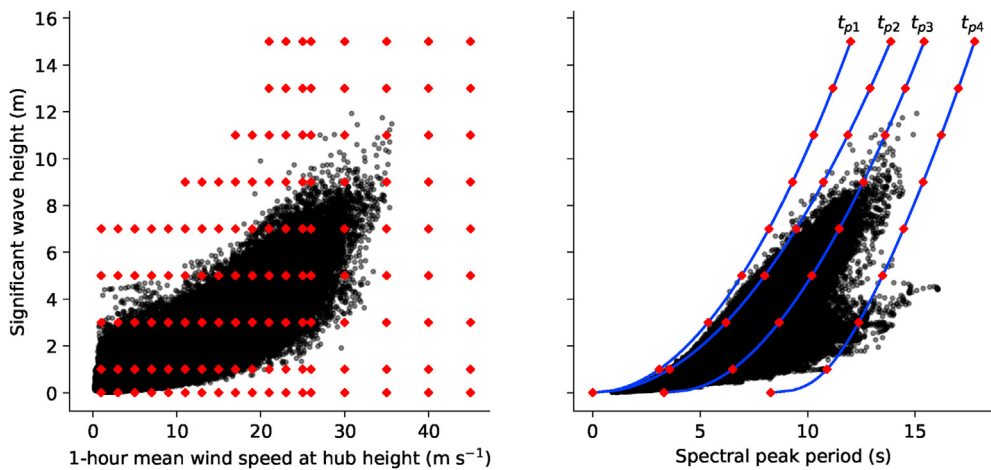


**Fig. 6.** Environmental conditions at which multiphysics simulations were performed and which were used to build the statistical response emulator (red diamonds). A total of 516 different environmental conditions were evaluated (129 wind speed - wave height combinations and for each wind - wave combination four different spectral peak period values;  $t_{p1}$ ,  $t_{p2}$ ,  $t_{p3}$ ,  $t_{p4}$ ). Black dots show the environmental conditions within the first 50 years of the dataset for the FINO 1 site.

used a block-maxima method, with  $F_{1h}$  modeled using the generalized extreme value (GEV) distribution. The location, scale, and shape parameters,  $(\mu, \sigma, \xi)$ , were modeled as parametric functions of wind speed, wave height and wave period. The cumulative distribution function for the 1-hour maximum response is then given by

$$F_{1h}(r|v, h_s, t_p) = \begin{cases} \exp\left(-\exp\left(-\frac{r-\mu}{\sigma}\right)\right), & \xi=0, \\ \exp\left(-\left(1+\xi\frac{r-\mu}{\sigma}\right)_+^{-1/\xi}\right), & \xi\neq0, \end{cases} \quad (3)$$

where  $(\cdot)_+ = \max\{\cdot, 0\}$ , and, for simplicity, the dependence of the parameters  $(\mu, \sigma, \xi)$  on  $(v, h_s, t_p)$  has not been written explicitly. Various methods can be used to estimate the models for  $(\mu, \sigma, \xi)$  as functions of  $(v, h_s, t_p)$ , such as radial basis function models or Gaussian process regression (Kriging). In this work we have opted to use simple parametric models. These models may not provide the optimal fit, but do allow the results of the study to easily be replicated. As described further below, the response emulator was found to be sufficiently representative for the purpose of the study. The fitted functions for  $\mu$ ,  $\sigma$  and  $\xi$  are given in the [supplemental material](#) and contain a total of 33 parameters.

The process to establish the response emulator involved the following steps:

1. 1-hour simulations were conducted across the wind speed, wave height, peak period variable space.
2. Each 1-hour simulation was divided into 1-min blocks (Fig. 7).
3. GEV distributions were fitted to the block maxima in each simulation.

4. The continuous dependence functions  $\mu(v, h_s, t_p)$ ,  $\sigma(v, h_s, t_p)$  and  $\xi(v, h_s)$  were fitted based on the various estimates of the parameters at discrete points of the variable space.
5. The 1-min maxima distribution was transformed into a 1-hour maxima distribution:  $F_{1h}(r) = [F_{1min}(r)]^{60}$ .

Fogle et al. [8] found that the maxima of 40–60 s blocks can be considered independent in wind turbine load responses. While we did not test for independence here, in some time series the 1-min maxima appear to be independent while other time series have some low-frequency modes that suggest that 1-min maxima are not truly independent.

The parameter values of the GEV vary across the variable space, with discontinuities at the cut-out wind speed (figures are shown in the [supplemental material](#)). While the estimates of the location and scale parameters vary relatively smoothly over the discrete simulation points, the shape parameter is more erratic, due to sampling variability.

The parametric response emulator captures important characteristics of the multiphysics simulations. This can be seen by

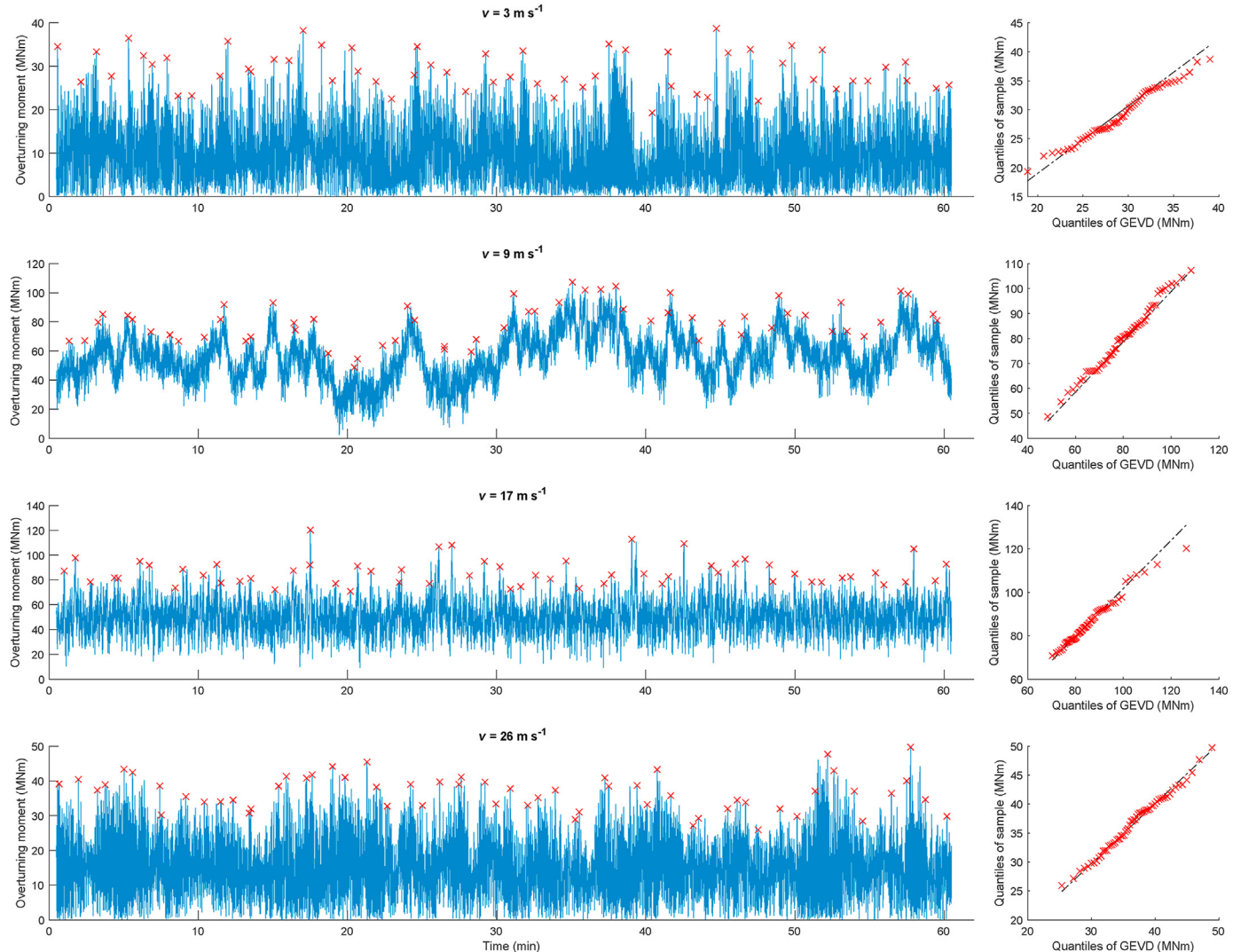


**Fig. 7.** Time series of hourly simulations at  $3, 9, 17$  and  $26 \text{ m s}^{-1}$  (from top to bottom) at a sea state of  $h_s = 1 \text{ m}$  and  $t_p = 6.51 \text{ s}$ . Red crosses represent the maxima of 1-min blocks. In the right panels quantile-quantile plots of the generalized extreme value distributions (GEVDs) that were fitted to the block maxima are shown.

comparing the GEV's parameter values over the variable space and by comparing realized 1-hour responses within the multiphysics simulations with random samples drawn from the emulator (Figs. 8–10). At calm sea ( $h_s = 0$  m), the multiphysics simulations describe a characteristic curve when the realized 1-hour maximum overturning moment is plotted over wind speed (see Fig. 8):

- The response increases roughly linearly until the rated wind speed of  $11.4 \text{ m s}^{-1}$ ,
- then it increases slower and with reduced short-term variability,
- at ca.  $17 \text{ m s}^{-1}$  the response starts to decrease with increasing wind speed, with high short-term variability, and
- finally, starting at  $25 \text{ m s}^{-1}$ , when the turbine switches into parked mode, the response drops and then increases quadratically with wind speed.

The response emulator reproduces these features of the response curve.

Overall, the response emulator for the overturning moment at 30 m water depth showed good agreement with the realizations of the multiphysics simulation. Differences were mostly below 20% (Fig. 9) and scatter plots suggested that there was no systematic over- or under-estimation from the emulator (Fig. 10).

In addition to the 30 m response emulator, we built an emulator for the bending moment at 10 m water depth. At 10 m water depth,

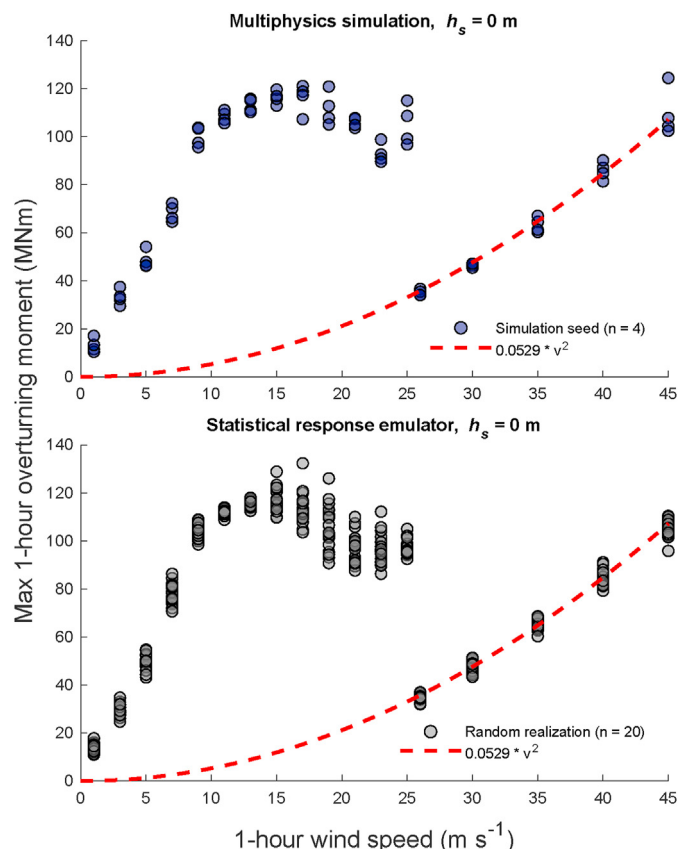


**Fig. 8.** Responses at different wind speeds during calm sea ( $h_s = 0$  m). Maxima from multiphysics simulations (top) and the response emulator (bottom) showed good qualitative agreement. The mudline overturning moment peaked during power production, but this peak would get exceeded at much higher wind speed during parked mode (ca.  $45\text{--}50 \text{ m s}^{-1}$ ). In parked mode the wind turbine did not vary its pitch angle anymore such that the overturning moment increases – like the drag force – with the square of the wind speed.

the wind's relative contribution is higher and the wave's relative contribution lower than at 30 m water depth. Thus, annual maxima of the 10 m moment can occur at different environmental conditions than annual maxima of the 30 m moment. The response emulator for the 10 m moment was defined based upon the 30 m emulator, assuming that wind and wave can be approximated as point forces at known heights (further details are given in the [supplemental material](#)). The median responses of both emulators are visualized in Fig. 11.

### 3.3. Isolating the effect of approximations in the environmental contour method

To isolate the effects of each approximation introduced in the environmental contour method, four quantities were derived from the 1000-year time series, corresponding to the 50-year responses estimated under various assumptions. For each 1-hour time step of the 1000-year series, both a stochastic and deterministic response was generated. The deterministic responses were calculated by always using the median short-term response instead of a random quantile. The 50-year responses for the stochastic and deterministic time series were then calculated either from the annual maxima, or from all hourly values, under the assumption of independence. In both cases, the empirical distribution derived from either the annual maxima or hourly values is used to calculate return values. The various return value estimates are denoted:

- $x_{s50}$ : calculated from annual maxima of the time series of stochastic responses
- $x_{d50}$ : calculated from annual maxima of the time series of deterministic responses
- $\bar{x}_{s50}$ : calculated from all hourly-maximum stochastic responses, under the assumption of independence
- $\bar{x}_{d50}$ : calculated from all hourly values of deterministic responses, under the assumption of independence

Under the assumption that the artificial time series and the response emulator represent reality, the estimator  $x_{s50}$  will be unbiased. It will have some degree of sampling uncertainty though as both, blocks of the artificial time series and hourly maximum responses given an environmental condition are sampled from distributions. For simplicity, we call  $x_{s50}$  the “true response”.

By comparing  $x_{s50}$  and  $\bar{x}_{s50}$  (or  $x_{d50}$  and  $\bar{x}_{d50}$ ), we can assess the impact of neglecting serial correlation in the metocean conditions. By comparing  $x_{s50}$  and  $x_{d50}$  (or  $\bar{x}_{s50}$  and  $\bar{x}_{d50}$ ), we can assess the impact of assuming a deterministic response. The impact of assuming a linearized failure surface and reducing the design problem to a 2D contour is assessed by comparing various contour-based response estimators: Two based on 2D IFORM contours [4], two based on 2D highest density contours [48] and one based on a 3D highest density contour. We denote these estimators as  $x_{c50}$ . The 2D contours were calculated from wind speed - wave height joint distributions and a fixed relationship for the peak period (or, equivalently, wave steepness) given a wind speed and wave height is assumed. For the 2D contours, the peak period associated with each design condition was calculated based on the observations with the highest 1% of significant wave height values for a given wind speed interval (see Fig. 12). Two different methods were used to establish a relation between steepness and wind speed for large values of significant wave height. In one case, the median steepness for the high  $H_s$  records was calculated as a function of wind speed. The empirical median values,  $s_{median}$ , were then approximated using the function

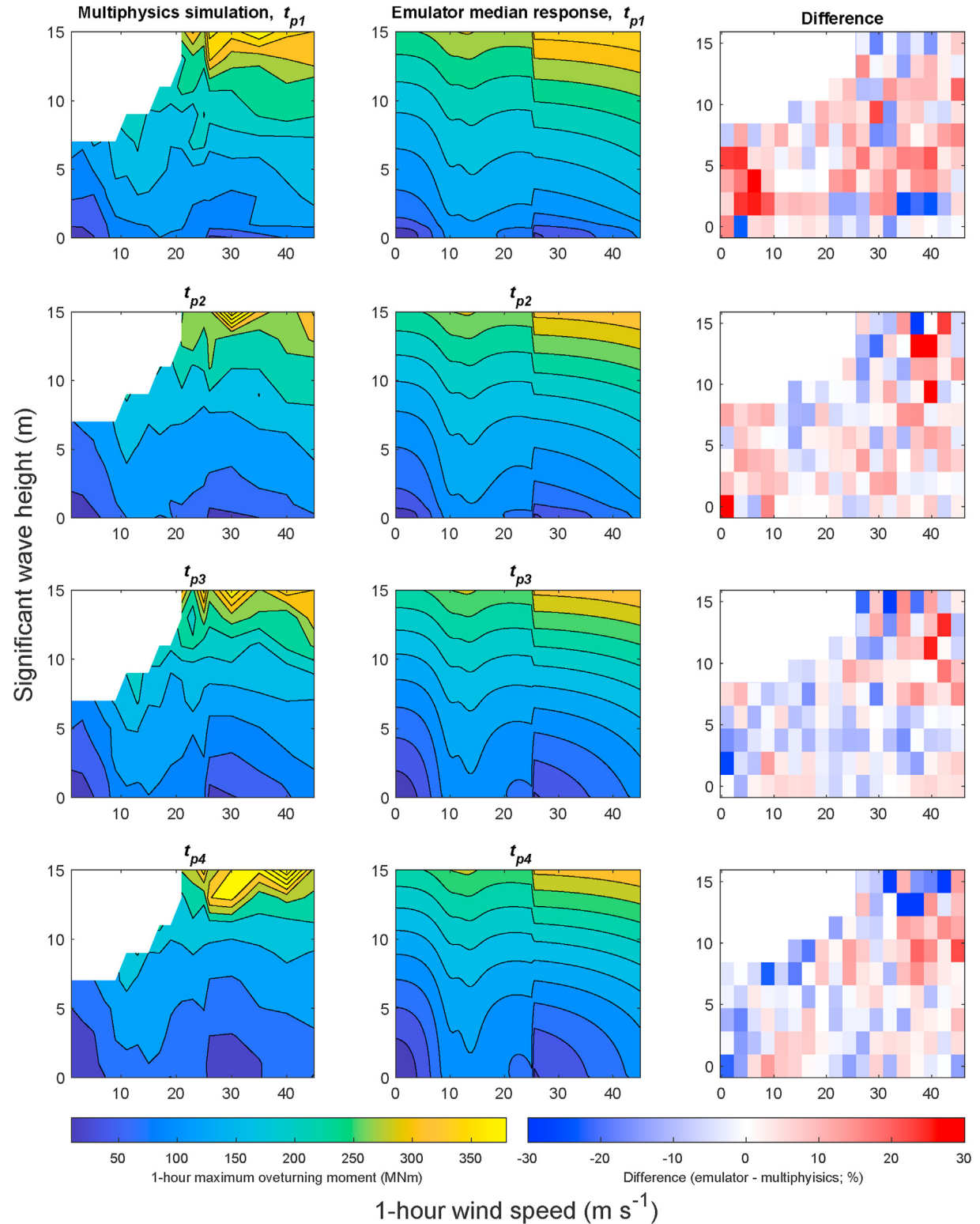


**Fig. 9.** Response across the wind speed - wave height variable space. Difference between the response from the multiphysics simulation and the emulator's median response predictions were below 20% for most environmental conditions.

$$s_{\text{median}} = 0.012 + \frac{0.0021}{1 + \exp[-0.3(v - 10)]}, \quad (4)$$

where steepness is calculated based on peak spectral period,  $t_p$ , and  $v$  is in  $\text{m s}^{-1}$ . In the other case, based on a visual inspection of the

data, the maximum steepness at a given wind speed and large  $H_s$  was approximated as

$$s_{\text{max}} = \begin{cases} 0.021 + 0.0017v & \text{if } v \leq 19 \text{ m s}^{-1} \\ 0.054, & \text{otherwise.} \end{cases} \quad (5)$$

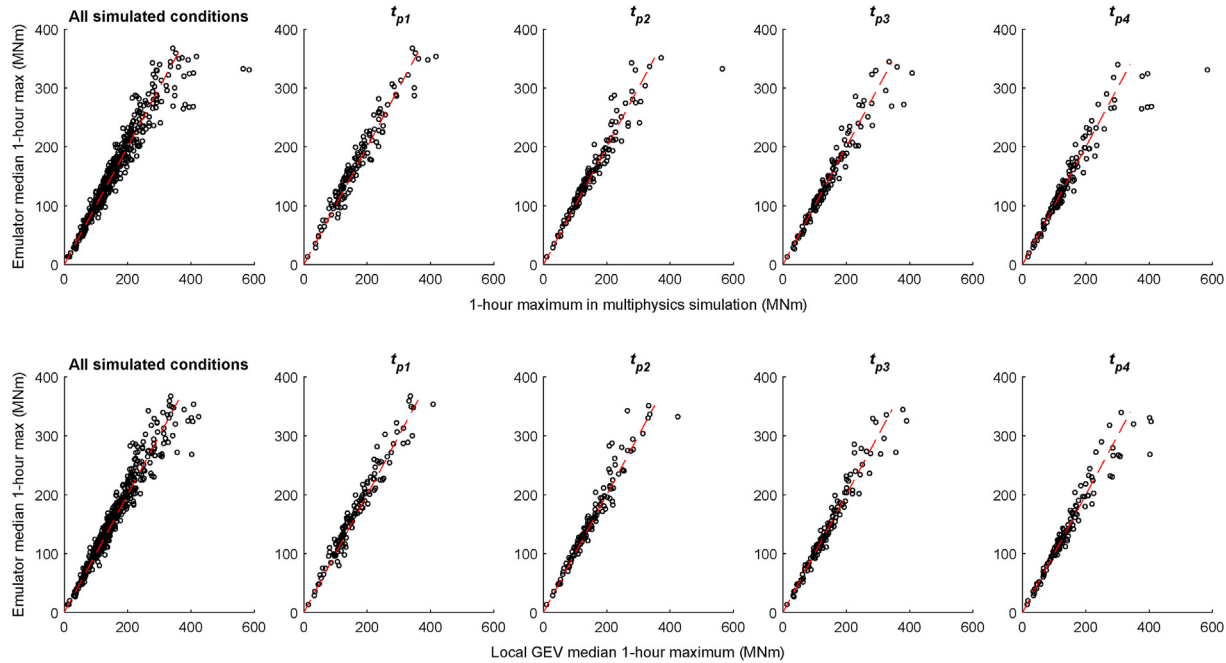


**Fig. 10.** Comparison between multiphysics simulations and the response emulator. Top: Median 1-hour maximum from emulator versus realized maximum in the multiphysics simulation. Bottom: Median 1-hour maximum from emulator versus median 1-hour maximum from the locally fitted generalized extreme value (GEV) distribution. Dashed lines represent perfect agreement between emulator and simulation.

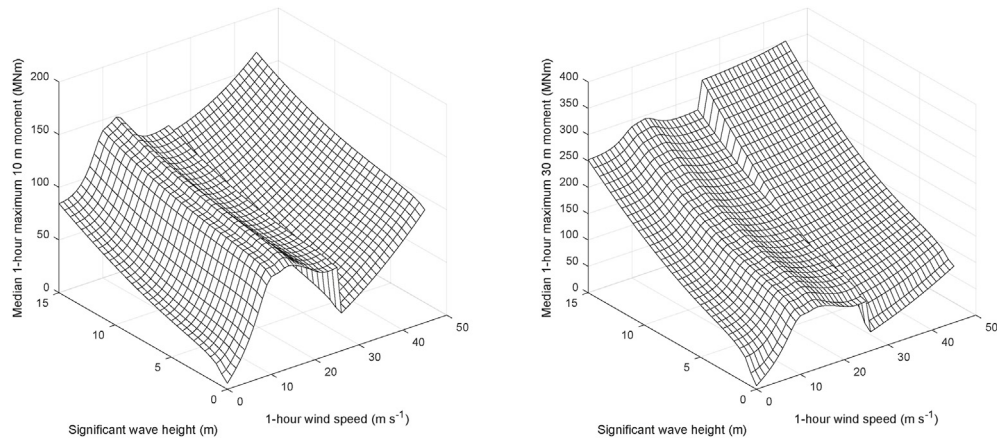


**Fig. 11.** Median response of the two statistical response emulators at  $t_p = t_{p2} = \sqrt{2\pi H_s/g} \cdot 0.04$  where  $g = 9.81 \text{ m s}^{-2}$ . At the cut-out wind speed of  $25 \text{ m s}^{-1}$  the responses have a discontinuity. There, the 10 m moment generally drops while the 30 m moment drops at low wave heights, but jumps at high wave heights.

Since the turbine's eigen period is around 3 s, for a given value of significant wave height and wind speed, sea states with higher steepness lead to larger loads. The contour estimates using  $s_{\max}$  will therefore be more conservative than those using  $s_{\text{median}}$ . However, since at this location the highest values of steepness tend to occur for lower values of  $H_s$  at a given wind speed (see Fig. 4), assuming that the highest loads occur along the environmental contour may not be conservative, since a lower value of  $H_s$  with a higher value of steepness may lead to larger loads in this case. This effect cannot be represented using the 2D contours, but can be accounted for using a 3D contour. For the 3D highest density contour, a deterministic relationship for  $T_p|V, H_s$  is not required, as the relation between the three variables is already specified by the contour.

The underlying joint distribution to calculate the contours was the empirical distribution, derived from an artificial time series with a length of ca. 2.5 million years, generated using the same

method used to generate the 1000-year times series. For all five contours, the estimate for the 50-year extreme moment was taken as the point along the contour that caused the highest response (using the response emulator).

#### 4. Results and discussion

Fig. 13 shows response time series for the 10 m and 30 m moment. In the top two panels the response is assumed to be deterministic (this is achieved by evaluating the response emulator at the 0.5 quantile at every time step) while in the bottom two panels the response is stochastic. In all cases the response time series has a roughly linear relationship with the wind speed time series if the wind speed is below ca.  $15 \text{ m s}^{-1}$ . As expected, the moment at 30 m water depth is higher than the moment at 10 m water depth.

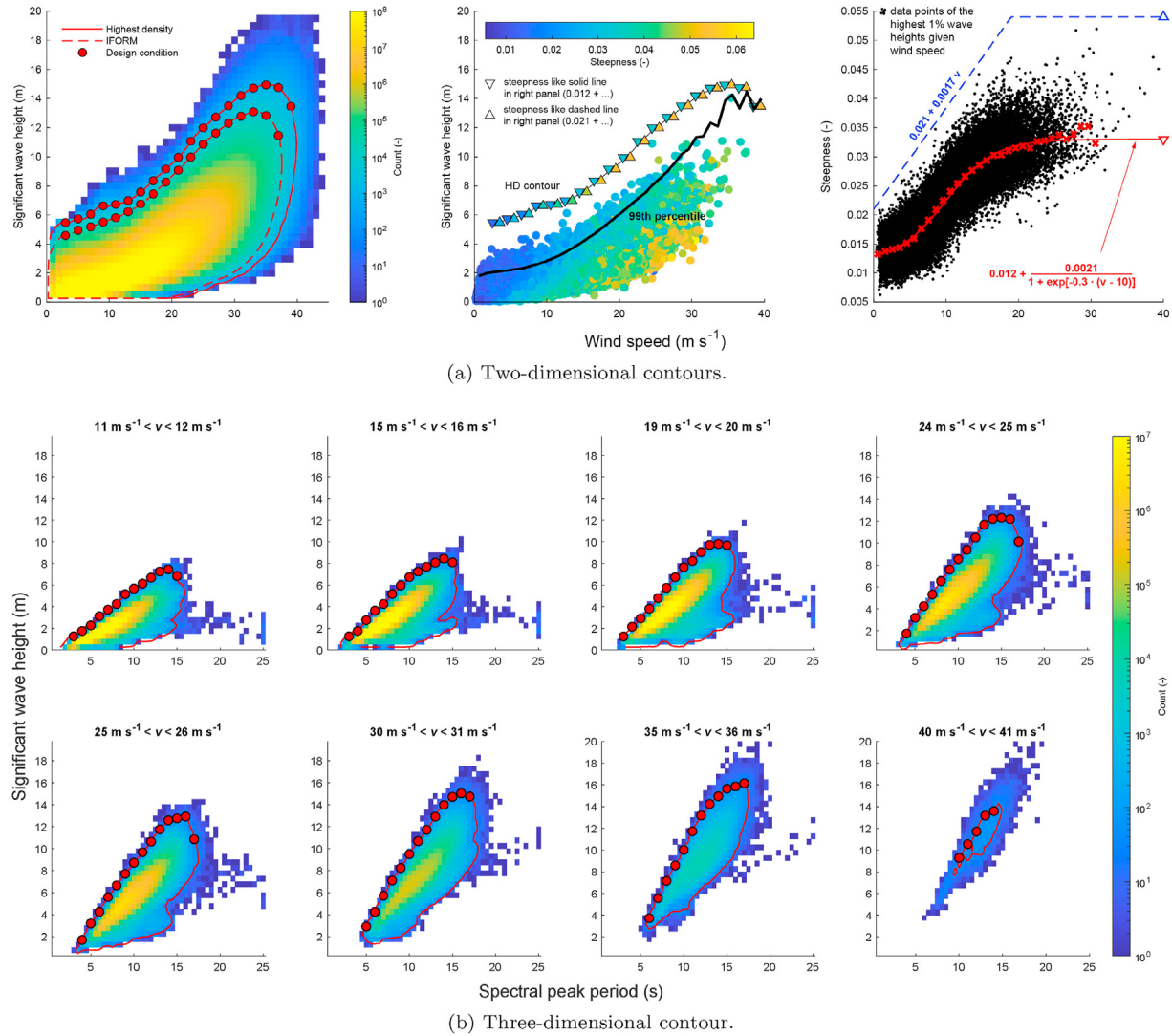


**Fig. 12.** 50-year environmental contours. The contours are based on the empirical distribution of an artificial time series with a length of ca. 2.5 million years. Design conditions are plotted as circles. (a) Two-dimensional IFORM and highest density contours. Two types of deterministic relationships for steepness conditional on wind speed were considered such that four different 2D contours were constructed. In the first type steepness was modeled as the median steepness of the highest 1% wave heights and in the second type it was modeled as the maximum steepness of the highest 1% wave heights (right panel). (b) Slices of the three-dimensional highest density contour. A threshold of 40 data points per cell defines the constant density contour.

While short periods of the four response time series showed similarities (Fig. 13), the annual maxima of the complete 1000-year time series have different characteristics (Fig. 14): Annual maxima of the 30 m moment are higher than annual maxima of the 10 m moment and have a greater variability. The 10 m moment annual maxima vary between ca. 110 and 130 MNm (deterministic) and ca. 130 and 180 MNm (stochastic), the 30 m moment annual maxima vary between 150 and 300 MNm (deterministic) and 180 and 420 MNm (stochastic). This difference can be explained by the type of wind-wave environmental conditions that cause the annual maxima. Fig. 15 shows the combinations of wind speed and significant wave height leading to the annual maximum bending moment at 10 m and 30 m, with the color denoting the corresponding size of the annual maximum value. The 10 m moment extremes are mostly caused by environmental conditions of medium wind speeds ( $13\text{--}20 \text{ m s}^{-1}$ ) during power production, but the largest values of the annual maximum 30 m moment are mostly caused by high wind speed – high wave height events when the turbine is shut down. The 50-year responses for the four considered

cases are listed in Table 4, as 114 MNm (10 m, deterministic), 252 MNm (30 m, deterministic), 158 MNm (10 m, stochastic) and 305 MNm (30 m, stochastic).

The different response characteristics also influence the accuracy of contour-based estimates. Lines of constant response of the 30 m moment show that there is only one region of high response along the IFORM contour (Fig. 16). For the 10 m response, however, there are two regions of high response along the contour and response lines at the level of the contour-based estimate are strongly non-convex. This suggests that contour-based estimates will be less conservative for the 10 m moment than they are for the 30 m moment. In particular, for IFORM contours, the assumption of a linearized failure surface is justified for the 30 m moment but is violated for the 10 m moment.

Fig. 17 shows the contours and the response values at their design conditions. When the short-term response was evaluated at the 0.5 quantile – as prescribed in the wind turbine design standard IEC 61400-3-1 [1] – all contour-based estimates of the 50-year 10 m moment,  $b_{50}$ , were lower than the true  $b_{50}$  value. For the

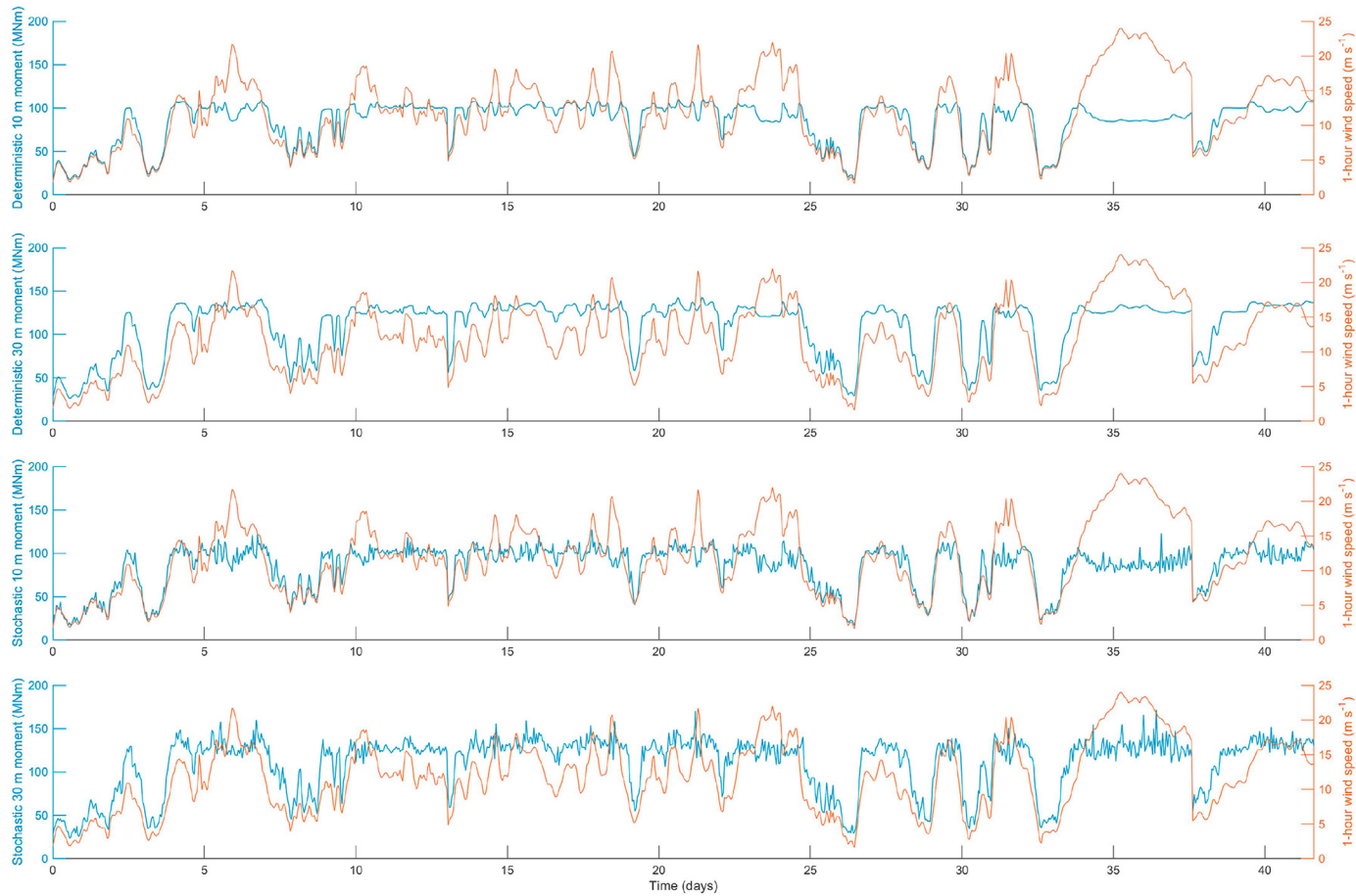


**Fig. 13.** Snippets of the hourly response time series simulated with the statistical response emulator for the moment at 10 m water depth and at 30 m water depth. Top two panels: Deterministic response (the emulator was evaluated at the 0.5 quantile). Bottom two panels: Stochastic response (the emulator was evaluated at random quantiles).

30 m moment, the two IFORM-based estimates were lower than the true  $r_{50}$  value while the highest density-based estimates were higher than the true value. While not prescribed in IEC's standard [1], for other marine structures, it is common practice to account for the response' short-term variability by evaluating the contour's design at a response quantile higher than 0.5. Which quantile needs to be chosen to account for short-term variability depends upon response characteristics of the application of interest. For example, Baarholm et al. [61] found that for the natural gas platform "troll A" the required quantile varied for the considered response variables, but was about 0.8.

Here, we found that for the 50-year 10 m moment,  $b_{50}$ , IFORM contours needed to be evaluated at the 0.99 quantile, 2D highest density contours at the 0.9 quantile and 3D highest density contours at the 0.8 quantile (Fig. 18). Note that this compensation did not only account for the effect of the response's short-term variability, but also balanced the effects of serial correlation and of contour construction: Contours were derived from the joint distribution of all 1-hour environmental conditions. Some of the environmental conditions that occurred at the tails of the joint distribution, however, were serially correlated, causing the contour to artificially inflate. Derbanne and de Hauteclocque [47] explain this effect and show de-clustering can be used to eliminate this effect. Contour construction is another source of bias: While IFORM contours use a non-conservative definition of exceedance for offshore wind turbines (due to the linearization of the failure surface), highest density contours use an overly conservative definition of exceedance (some of the datapoints that are counted as

exceedance do not lead to failure-relevant loads). The effect of the type of contour on the conservatism is discussed in Refs. [6,60].

The effect of the contour type (IFORM, highest density, steepness assumption) can be better analyzed if short-term variability is "turned off". Thus, we can compare contour-based estimates with FLTA based estimates where the short-term response is deterministic. As contours are derived from the serially correlated hourly data, an appropriate comparison is the 50-year quantile from the continuous 1000-year deterministic response time series. This quantile is also affected by serial correlation, but not by the response's short-term variability. For the 10 m moment, this estimate is 119 MNm. When the median steepness value is used, the IFORM-based estimate is 114 MNm and the HD-based estimate is 133 MNm (Table 4). Thus, as expected, IFORM's definition of exceedance is non-conservative while's HD's definition of exceedance is overly conservative. This comparison also suggests that using the median steepness of the highest 1% of waves at a given wind speed is conservative enough because when the maximum steepness is used the IFORM-based estimate is 119 MNm, which is the same as the estimate from the 1000-year time series. We know, however, that by IFORM's contour construction definition, we should get a response less than 119 MNm. Thus, in the maximum steepness case IFORM's non-conservative exceedance definition is balanced by the overly conservative assumption of a too high steepness value and consequently a too low spectral peak period value.

The different types of biases are visualized in Fig. 19. They comprise bias due to contour construction, due to serial correlation and due to short-term variability. The analysis shows that bias due

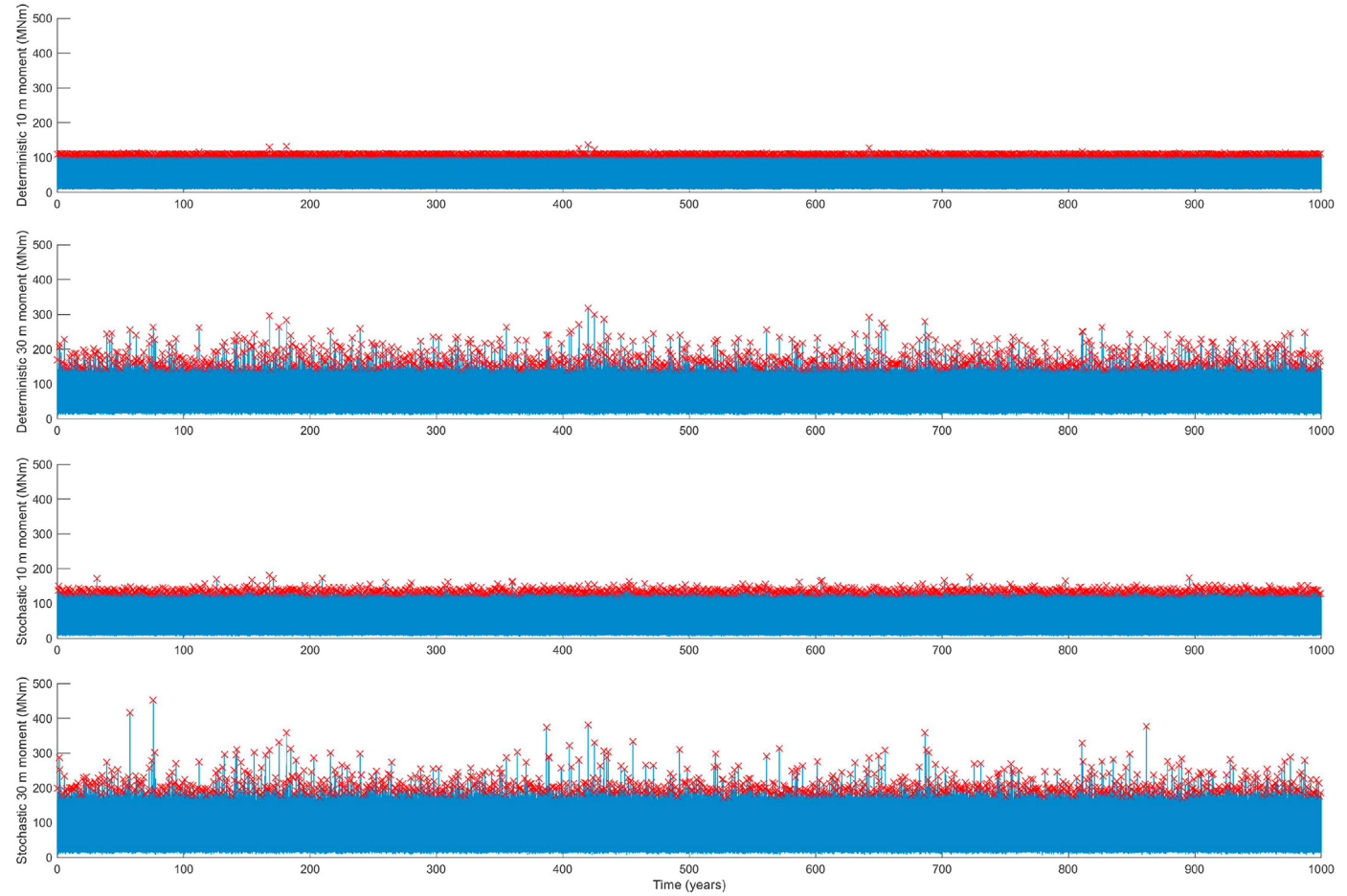


**Fig. 14.** Full 1000-year response time series (moment at 10 m water depth and at 30 m water depth). Top two panels: Deterministic response (the emulator was evaluated at the 0.5 quantile). Bottom two panels: Stochastic response (the emulator was evaluated at random quantiles). Red crosses represent annual maxima.

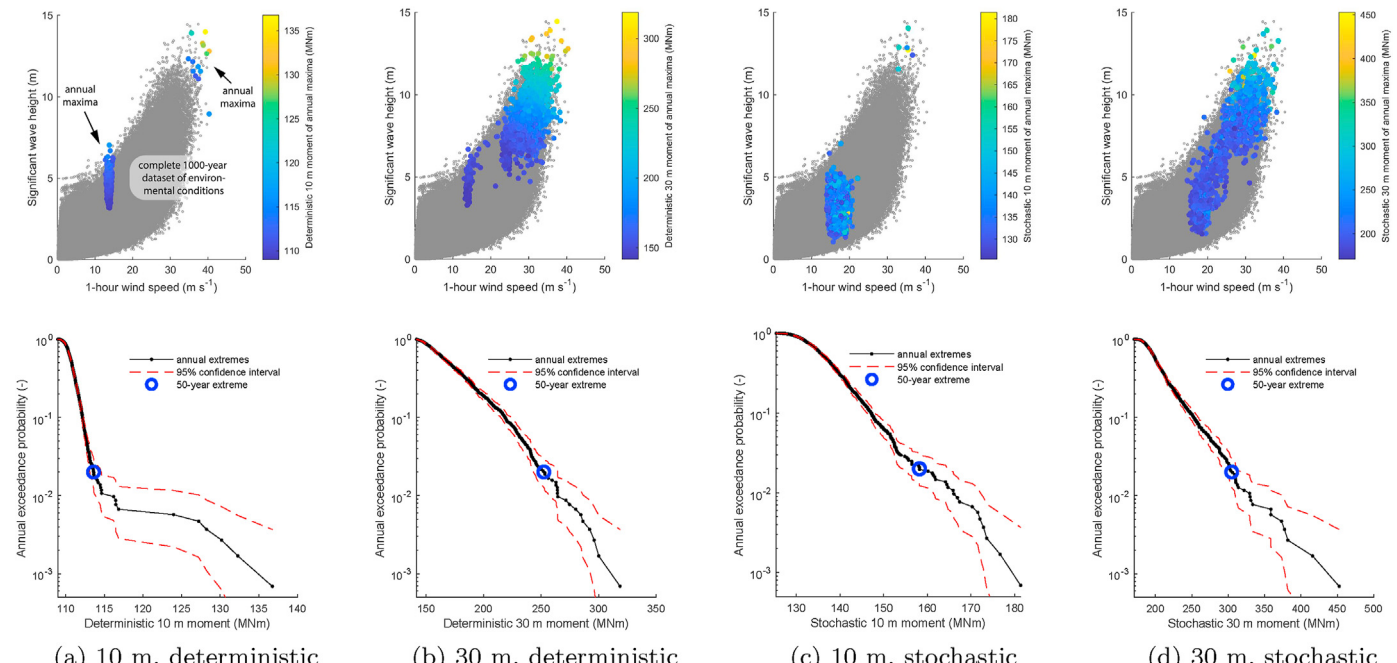


**Fig. 15.** Top row: Combinations of wind speed and significant wave height where the annual maximum bending moments occurred in the 1000-year time series. Color of points indicates corresponding annual maximum load. Bottom row: Exceedance probability of annual maximum moment.

**Table 4**

Comparison of estimates for the 50-year extreme moment at 10 and 30 m water depth ( $b_{50}$  and  $r_{50}$ , respectively). The contour-based estimates were calculated by evaluating the short-term response at the 0.5 quantile.  $b_{50}^*$  and  $r_{50}^*$  are the estimated 50-year moments normalized by the true 50-year moments at 10 and 30 m water depth, respectively.

Method	$b_{50}$ (MNm)	$b_{50}^*$ (-)	$r_{50}$ (MNm)	$r_{50}^*$ (-)
Annual maxima of 1000-year time series with a stochastic short-term response ("true"), $x_{s50}$	158	1.000	305	1.000
Annual maxima of 1000-year time series with a deterministic short-term response, $x_{d50}$	114	0.721	252	0.827
Continuous 1000-year response time series with a stochastic short-term response, $\bar{x}_{s50}$	158	1.000	312	1.025
Continuous 1000-year response time series with a deterministic short-term response, $\bar{x}_{d50}$	119	0.752	276	0.905
2D IFORM contour with median steepness	114	0.722	281	0.921
2D IFORM contour with high steepness	119	0.750	292	0.957
2D HD contour with median steepness	133	0.843	329	1.080
2D HD contour with high steepness	137	0.867	339	1.111
3D HD contour	141	0.889	358	1.174

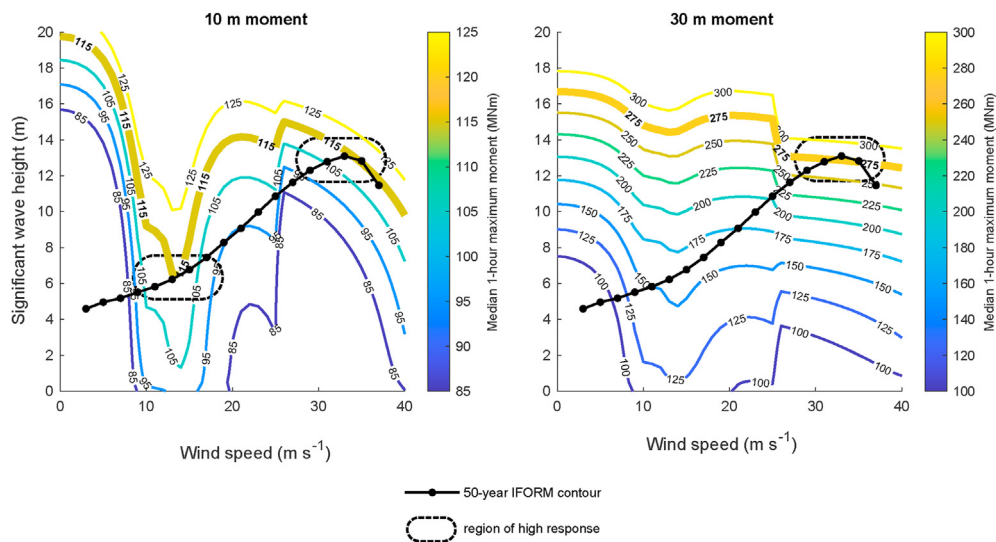


**Fig. 16.** Lines of constant response and IFORM contour. The extreme response of the 30 m water depth moment is dominated by high wind speed – high wave height events while the extreme response of the 10 m water depth moment is influenced by both, mid wind speed and high wind speed events. The IFORM contour's assumption of a single linearized failure surface roughly holds at 30 m water depth, but is violated at 10 m water depth because the failure surface has two "regions of high response" along the environmental contour. Spectral peak period was calculated according to Equation (4).

to contour construction can lead to an under- or overestimation of the response. The bias due to serial correlation always leads to an overestimation and the bias due to neglecting short-term variability always leads to an underestimation. As a consequence, overall bias can be positive or negative.

The biggest source of bias in the estimate of  $b_{50}$  is due to the response's short-term variability. Because contour design conditions are evaluated at a single short-term response quantile, they have a negative bias due to ignoring short-term variability. In principle, the total bias – the sum of contour construction, serial correlation and short-term variability bias – can be compensated by evaluating the contour's design condition at a higher quantile of the short-term response. However, there is no theoretical support for compensating the bias due to contour construction and due to serial correlation by evaluating the short-term response at a higher quantile. If the bias effect is taken into account, it would be more logical to compensate the biases of contour construction and serial correlation by inflating or deflating the contour. An IFORM contour is too small if the failure surface is non-convex (as is the case here) and a contour based on serially correlated environmental data is too big.

The results of this study are sensitive to the response and to the environment. While we aimed to build a high-quality response emulator and a high-quality statistical model to produce artificial time series, two particular aspects might deviate from reality: The

response emulator's GEV distribution's shape parameter is positive at medium wind speeds of about  $18 \text{ m s}^{-1}$ , which means that the distribution does not have an upper bound. In reality, there is an upper bound. Thus, the estimated distribution has some bias in the tail. By performing multiphysics simulations longer than 1 hour and possibly using the maxima from blocks longer than 1 min one could estimate the tail better. Another possible bias is our model for the distribution of significant wave height. Given that the considered site has a water depth of 30 m, the model might overestimate the occurrence of very high wave heights. Both aspects are important because for some response variables the extremes occur at the mid-wind speed region and for other variables they occur at the high wind speed – high wave height region. If the response at mid wind speeds is different or the environment at high wind speeds, the differences between the true 50-year response and the contour-based estimate could change.

Similarly, that means that the results are sensitive if a different response variable is analyzed that we did not consider here or if a different offshore site is analyzed. Some results, however, likely hold for other response variables and other offshore sites:

1. Due to a wind turbine's controller, there will always be response variables where the contour has two regions of high response in the wind speed – significant wave height variable space, which implies a non-convex failure surface. Therefore, the IFORM

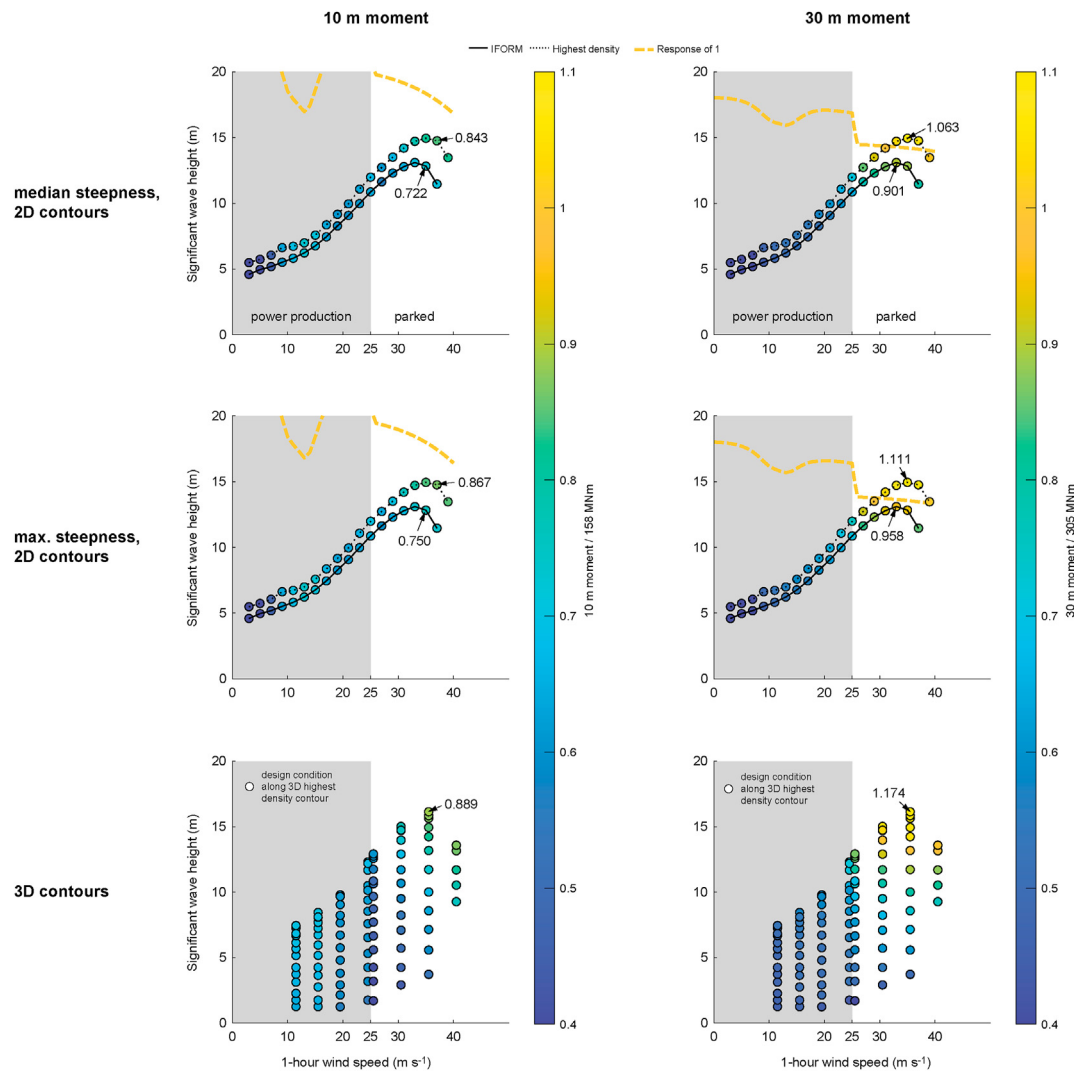


**Fig. 17.** Response at the contours' design conditions normalized by the true 50-year response. Design conditions were evaluated at the 0.5 quantile.

approximation of a linearized failure surface is non-conservative in this application. To avoid this source of non-conservatism, an ISORM or highest density contour can be constructed instead. However, if spectral peak period is varied deterministically with  $H_s$  and  $V$ , this relationship can offset the non-conservatism of the IFORM contour.

2. Serial correlation leads to an overestimation of the contour-based estimate. In this study the effect was up to 8%.
3. The response short-term variability leads to an underestimation of the contour-based estimate. In this study the effect was between 17 and 28%.
4. If there is a clear understanding, which spectral peak periods cause an unfavorable response, a 2D wind speed - wave height contour can be used instead of a 3D contour, together with a typical unfavorable  $T_p$  value. Although such probabilistic-deterministic variable combinations are theoretically fuzzy, they greatly reduce the number of design conditions along the "contour" that need to be evaluated. If there is no clear understanding about which  $T_p$  values are unfavorable, a 3D "contour" should be constructed.

These four points might help designers of wind turbines deal with the effects of the various assumptions in environmental contour methods. Because individual errors can either add up or

balance each other out, understanding the sources of bias is of great practical importance.

Future research on the long-term response of offshore wind turbines could explore other response variables and other sites. It would be interesting to explore the upper bound of bias for contour-based estimates. Additionally, future research could explore how more environmental variables could be considered during the estimation of the long-term response. Implicitly, we assumed in this study that only wind speed, significant wave height and spectral peak period change over time. This means that we assumed that wind and wave always come from the same direction and that sea level, current, turbulence structure, spectrum type and many other variables are constant. At the moment, it is unclear how big the influence of this assumption is. Other variables could be incorporated into either FLTA or contour-based estimates. However, estimating joint distributions and conducting a sufficient number of response simulations, becomes problematic as the number of variables increases.

## 5. Conclusions

In this work, we analyzed how well the long-term extreme response of an offshore wind turbine can be estimated based on environmental contours. The question was motivated by the fact

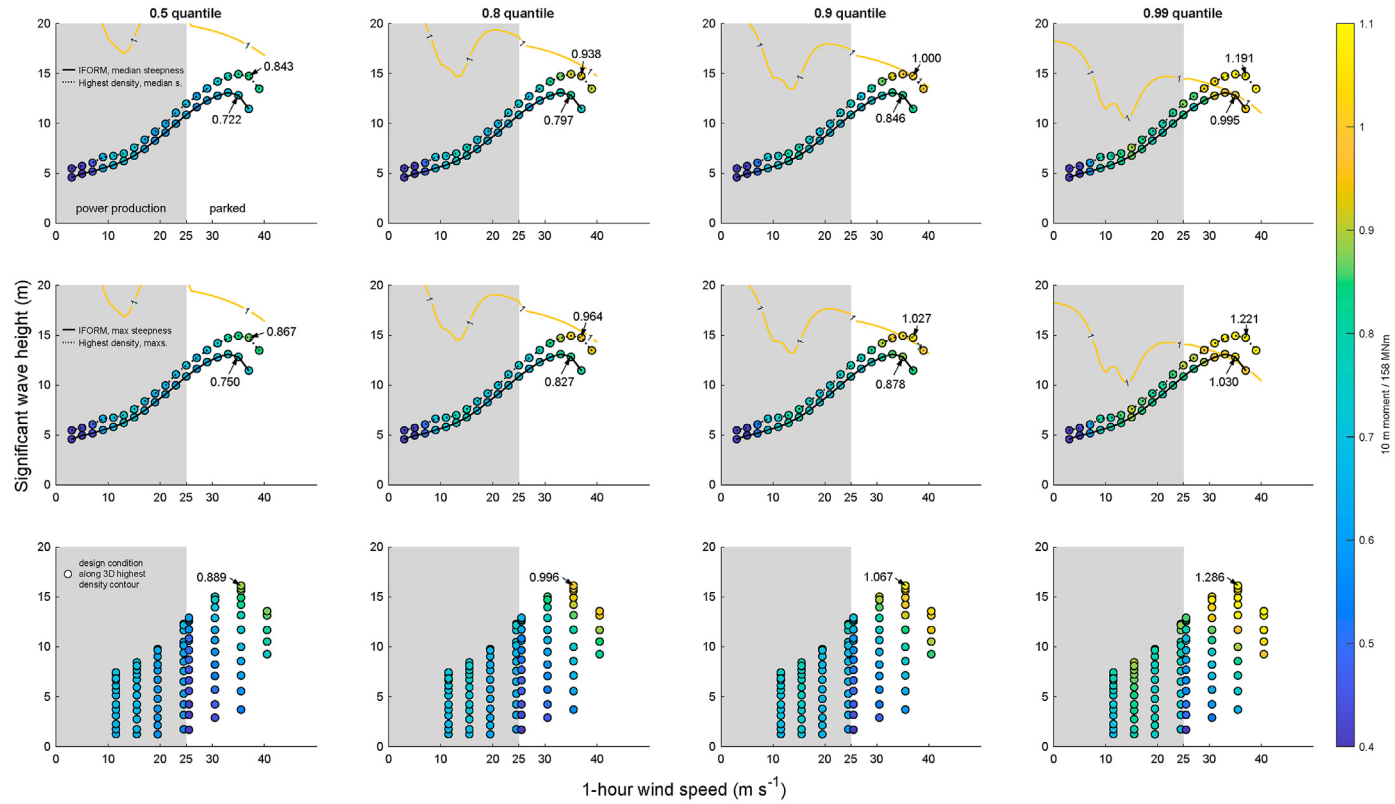


**Fig. 18.** 10 m moment at the contours' design conditions normalized by the true 50-year response. The design conditions are evaluated at various quantiles of the short-term response.

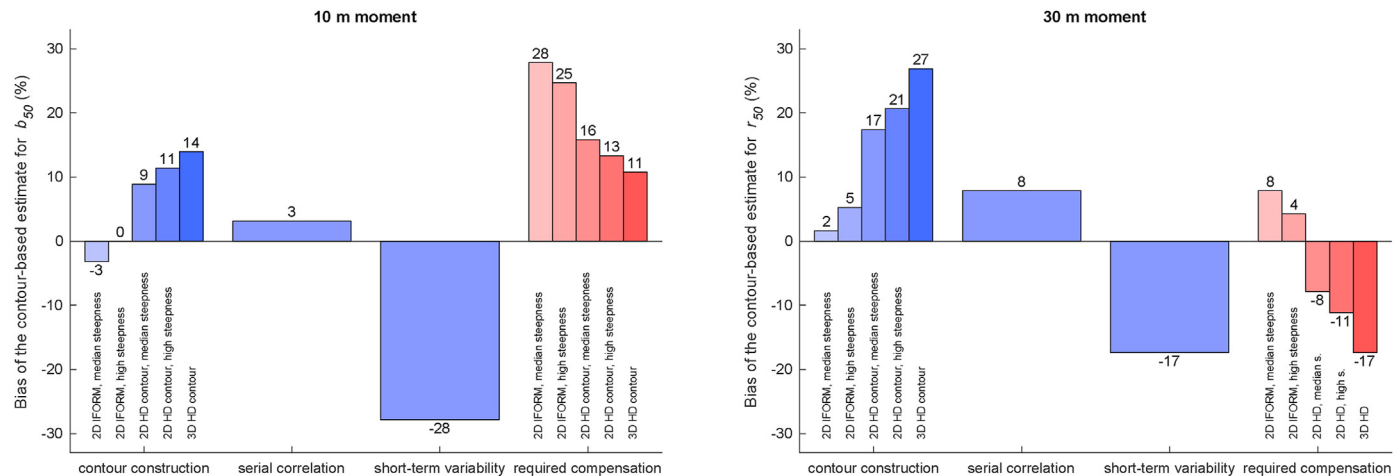


**Fig. 19.** Sources of bias for the two contour-based estimates, the 50-year 10 m moment (a) and the 50-year 30 m moment (b). Contour construction bias can be negative or positive, however, serial correlation bias is always positive and short-term variability bias is always negative. The contour's design condition were evaluated at the 0.5 quantile of the short-term response. Contour construction bias:  $x_{c50} - \bar{x}_{d50}$ , serial correlation bias:  $\bar{x}_{d50} - x_{d50}$ , short-term variability bias:  $x_{d50} - x_{s50}$ , overall required compensation:  $x_{s50} - x_{c50}$ . Definitions for these variables are given in subsection 3.3.

that authoritative design standards recommend the use of environmental contours for wind turbine design, however, it was unclear how these contour-based estimates compare to the true long-term response. Offshore wind turbine design is particularly concerned with the 50-year extreme response. As estimating the true 50-year extreme response with high accuracy requires the characterization of the response over at least one order of magnitude longer time periods than the return period of interest, we used a statistical response emulator for the short-term response and a statistical model to generate environmental data of arbitrary lengths.

A high-accuracy estimate of the response was obtained by simulating the short-term response of continuous 1000-year artificial time series using a response emulator. The emulator was previously created based on multiphysics simulations that were performed across the complete wind-wave variable space. We considered five different environmental contours, including the approach that is currently recommended in the design standard IEC 61400-3-1 [1]. We found that – as already suggested by other authors – the recommended IFORM contour approach can underestimate the response to some degree because it assumes a convex

failure surface. However, this effect was only apparent in some response variables such as the 10 m moment, but it did not play a role in others such as the 30 m moment. In addition, the effect was relatively small in the affected response variables. Other sources of bias of the contour-based estimates were serial correlation and short-term variability. For the 10 m moment short-term variability was by far the strongest source of bias. The broader literature on marine structures proposed to compensate for this effect by evaluating the contour's design condition at a higher quantile of the short-term response. Currently, this is not mentioned in the wind turbine design standard [1], which recommends to use the average of the maxima of several stochastic realizations. For a symmetric distribution this is equivalent with evaluating the distribution of the maxima of the short-term response at the 0.5 quantile, in other words, taking the median maximum. Here, we found that this could dramatically underestimate the true 50-year response. For the 50-year extreme of the moment at 10 m water depth the design conditions needed to be evaluated at the 0.99 quantile to compensate the bias as otherwise the true response was underestimated by 25–28% (depending upon which relationship for  $T_p|V, H_s$  was considered). Alternatively, if a highest density contour were used instead of an IFORM contour, its design conditions needed to be evaluated at the 0.9 quantile to compensate for the bias.

The differences between contour-based estimates and the true 50-year return values, however, were very sensitive to the type of response (moment at 30 m water depth or moment at 10 m water depth) and are likely also very sensitive to the offshore site: The turbine's controller succeeds in pitching the blades to reduce loads as wind speeds increase, however, as a side-effect long-term extremes might occur during power production or during parked condition – depending upon the response variable and the site's environmental conditions. This makes estimating the extreme response based on an environmental contour particularly challenging as the response's short-term variability at these two states can be very different. Thus, the bias in a contour-based estimate due to short-term variability can vary depending on the response variable and offshore site characteristics. The full long-term analysis used in this work can be used to calculate an unbiased estimator of the long-term extreme response and to identify the different sources of bias associated with a contour-based estimate.

## Data availability

The artificial time series and the results of the multiphysics simulation are available as a Zenodo repository at <https://doi.org/10.5281/zenodo.5013306>. The scripts that were used in the analysis of this study are available as a GitHub repository at <https://github.com/ahaselsteiner/2021-extreme-response>.

## Contributions

AFH and EM conceptualized this study. MF performed the multiphysics simulations, with support from AS and AFH. EM developed the environmental model and generated the artificial time series. AFH developed the response emulator. AFH lead the analysis and writing of the paper. AFH, EM, AS and MF edited and revised the original draft. KDT provided supervision.

## Declaration of competing interest

The authors declare that they have no known competing financial interests or personal relationships that could have appeared to influence the work reported in this paper.

## Acknowledgements

We thank Jason Jonkman for helping with questions concerning openFAST. EM was funded by the UK EPSRC Supergen Offshore Renewable Energy Hub [grant no: EP/S000747/1] Flexible Fund project "Improved Models for Multivariate Metocean Extremes (IMEX)".

## Appendix A. Supplementary data

Supplementary data to this article can be found online at <https://doi.org/10.1016/j.renene.2021.09.077>.

## References

- [1] International Electrotechnical Commission, Wind Energy Generation Systems - Part 3-1: Design Requirements for Fixed Offshore Wind Turbines, 2019. Tech. Rep. IEC 61400-3-1.
- [2] A. Morató, S. Sriramula, N. Krishnan, J. Nichols, Ultimate loads and response analysis of a monopile supported offshore wind turbine using fully coupled simulation, Renew. Energy 101 (2017) 126–143, <https://doi.org/10.1016/j.renene.2016.08.056>.
- [3] S. Haver, Wave climate off northern Norway, Appl. Ocean Res. 7 (2) (1985) 85–92, [https://doi.org/10.1016/0141-1187\(85\)90038-0](https://doi.org/10.1016/0141-1187(85)90038-0).
- [4] S.R. Winterstein, T.C. Ude, C.A. Cornell, P. Bjerager, S. Haver, Environmental parameters for extreme response: inverse FORM with omission factors, in: Proc. 6th International Conference on Structural Safety and Reliability (ICOSSAR 93), Innsbruck, Austria, 1993.
- [5] E. Ross, O. C. Astrup, E. Bitner-Gregersen, N. Bunn, G. Feld, B. Gouldby, A. Huseby, Y. Liu, D. Randell, E. Vanem, P. Jonathan, On environmental contours for marine and coastal design, Ocean Eng. doi: 10.1016/j.oceaneng.2019.106194 .
- [6] E. Mackay, A. F. Haselsteiner, Marginal and total exceedance probabilities of environmental contours, Mar. Struct. 75, doi: 10.1016/j.marstruc.2020.102863 .
- [7] P.M. Videiro, T. Moan, Efficient evaluation of long-term distributions, in: Proc. 18. International Conference on Offshore Mechanics and Arctic Engineering, OMAE99), 1999.
- [8] J. Fogle, P. Agarwal, L. Manuel, Towards an improved understanding of statistical extrapolation for wind turbine extreme loads, Wind Energy 11 (6) (2008) 613–635, <https://doi.org/10.1002/we.303>.
- [9] L.V. Sagrilo, A. Naess, A.S. Doria, On the long-term response of marine structures, Appl. Ocean Res. 33 (2011) 208–214, <https://doi.org/10.1016/j.apor.2011.02.005>.
- [10] A. Naess, T. Moan, Stochastic Dynamics of Marine Structures, Cambridge University Press, Cambridge, United Kingdom, 2013, <https://doi.org/10.1017/CBO9781139021364>.
- [11] K. Saranyasoontorn, L. Manuel, On assessing the accuracy of offshore wind turbine reliability-based design loads from the environmental contour method, Int. J. Offshore Polar Eng. 15 (2) (2006) 132–140. ISSN 1053-5381.
- [12] Q. Li, Z. Gao, T. Moan, Modified environmental contour method for predicting long-term extreme responses of bottom-fixed offshore wind turbines, Mar. Struct. 48 (2016) 15–32, <https://doi.org/10.1016/j.marstruc.2016.03.003>. ISSN 09518339.
- [13] J.-T. Horn, S. R. Winterstein, Extreme response estimation of offshore wind turbines with an extended contour-line method, J. Phys. Conf. 1104, doi: 10.1088/1742-6596/1104/1/012031 ..
- [14] J. Velarde, E. Vanem, C. Kramhöft, J. Dalsgaard, Probabilistic analysis of offshore wind turbines under extreme resonant response: application of environmental contour method, Appl. Ocean Res. 93 (2019), <https://doi.org/10.1016/j.apor.2019.101947>, 101947–1 to 101947–16.
- [15] E. Mackay, P. Jonathan, Sampling properties and empirical estimates of extreme events, Ocean Engineering 239 (2021) 109791, <https://doi.org/10.1016/j.oceaneng.2021.109791>.
- [16] E. Mackay, P. Jonathan, Sampling properties and empirical estimates of extreme events, Ocean Engineering (accepted) URL <http://www.lancs.ac.uk/~jonathan/MckInt21.pdf>.
- [17] G.Z. Forristall, How should we combine long and short term wave height distributions?, in: Proc. 27th International Conference on Offshore Mechanics and Arctic Engineering (OMAE 2008) American Society of Mechanical Engineers (ASME), 2008.
- [18] E. Mackay, L. Johanning, Long-term distributions of individual wave and crest heights, Ocean Eng. 165 (2018) 164–183, <https://doi.org/10.1016/j.oceaneng.2018.07.047>.
- [19] H.O. Madsen, S. Krenk, N.C. Lind, Methods of Structural Safety, Prentice-Hall, Englewood Cliffs, NJ, USA, 1986.
- [20] F.I.G. Giske, B.J. Leira, O. Øiseth, Full long-term extreme response analysis of marine structures using inverse FORM, Probabilist. Eng. Mech. 50 (2017) 1–8, <https://doi.org/10.1016/j.probengmech.2017.10.007>.

- [21] F. I. G. Giske, B. J. Leira, O. Øiseth, Long-term extreme response analysis of marine structures using inverse SORM, *J. Offshore Mech. Arctic Eng.* 140 (5), ISSN 1528896X, doi: 10.1115/1.4039718 ..
- [22] N. Nordenström, *Methods for Predicting Long Term Distributions of Wave Loads and Probability of Failure for Ships*, Det Norske Veritas, 1969. Tech. Rep., DNV report no. 69-21-S.
- [23] J. Battjes, *Long-term Wave Height Distribution at Seven Stations Around the British Islands*, Tech. Rep., National Institute of Oceanography, 1970.
- [24] M.J. Tucker, An improved 'Battjes' method for predicting the probability of extreme waves, *Appl. Ocean Res.* 11 (4) (1989) 212–218, [https://doi.org/10.1016/0141-1187\(89\)90020-5](https://doi.org/10.1016/0141-1187(89)90020-5).
- [25] C. Guedes Soares, Long term distribution of non-linear wave induced vertical bending moments, *Mar. Struct.* 6 (1993) 475–483, [https://doi.org/10.1016/0951-8339\(93\)90033-Y](https://doi.org/10.1016/0951-8339(93)90033-Y).
- [26] A. Naess, Technical note: on the long-term statistics of extremes, *Appl. Ocean Res.* 6 (4) (1984) 227–228, [https://doi.org/10.1016/0141-1187\(84\)90061-0](https://doi.org/10.1016/0141-1187(84)90061-0). ISSN 01411187.
- [27] H.E. Krogstad, Height and period distributions of extreme waves, *Appl. Ocean Res.* 7 (3) (1985) 158–165, [https://doi.org/10.1016/0141-1187\(85\)90008-2](https://doi.org/10.1016/0141-1187(85)90008-2).
- [28] P.J. Moriarty, W.E. Holley, S. Butterfield, Extrapolation of Extreme and Fatigue Loads Using Probabilistic Methods, URL, National Renewable Energy Laboratory (NREL), 2004. Tech. Rep., <http://www.nrel.gov/docs/fy05osti/34421.pdf>.
- [29] M.J. Muliawan, Z. Gao, T. Moan, Application of the contour line method for estimating extreme responses in the mooring lines of a two-body floating wave energy converter, *J. Offshore Mech. Arctic Eng.* 135 (2013), <https://doi.org/10.1115/1.4024267>, 031301–1 to 031301–10.
- [30] P.M. Videiro, J.S. Monsalve Giraldo, F.J. Mendes de Sousa, C.M. Peri Machado dos Santos, L.V.S. Sagrilo, Long-term analysis using a scatter diagram key region to evaluate the extreme response of steel risers, *Mar. Struct.* 64 (2019) 322–340, <https://doi.org/10.1016/j.marstruc.2018.11.011>.
- [31] O. Gramstad, C. Agrell, E. Bitner-Gregersen, B. Guo, E. Ruth, E. Vanem, Sequential sampling method using Gaussian process regression for estimating extreme structural response, ISSN 09518339, *Mar. Struct.* 72 (April) (2020) 102780, <https://doi.org/10.1016/j.marstruc.2020.102780>.
- [32] P. Marshall, M. Rezvan, A. Gunatunga, Response based criteria for west of Shetlands, *J. Offshore Technol.* 3 (2) (1995) 42–45.
- [33] R. G. Standing, R. Eichaker, H. D. Lawes, B. Campbell, R. B. Corr, Benefits of applying response-based design methods to deepwater FPSOs, Proceedings of the Annual Offshore Technology Conference doi: 10.4043/14232-ms ..
- [34] S. Mazaheri, M.J. Downie, Response-based method for determining the extreme behaviour of floating offshore platforms, *Ocean Eng.* 32 (2005) 363–393, <https://doi.org/10.1016/j.oceaneng.2004.08.004>.
- [35] E. Fontaine, P. Orsero, A. Ledoux, R. Nerzic, M. Prevosto, V. Quiniou, Reliability analysis and response based design of a moored FPSO in West Africa, *Struct. Saf.* 41 (2013) 82–96, <https://doi.org/10.1016/j.strusafe.2012.08.002>.
- [36] E. Vanem, B. Guo, E. Ross, P. Jonathan, Comparing different contour methods with response-based methods for extreme ship response analysis, *Mar. Struct.* 69, doi: 10.1016/j.marstruc.2019.102680 ..
- [37] A. Brown, W. Gorter, P. Tromans, P. Jonathan, P. Verlaan, Design approach for turret moored vessels in highly variable squall conditions, in: Proc. 36th International Conference on Ocean, Offshore and Arctic Engineering (OMAE 2017), American Society of Civil Engineers, 2017, <https://doi.org/10.1115/OMAE2017-61005>.
- [38] H. F. Hansen, D. Randell, A. R. Zeeberg, P. Jonathan, Directional–seasonal extreme value analysis of North Sea storm conditions, *Ocean Eng.* 195, doi: 10.1016/j.oceaneng.2019.106665 ..
- [39] E.B. Mackay, P. Jonathan, Estimation of environmental contours using a block resampling method, in: Proc. 39th International Conference on Ocean, Offshore and Arctic Engineering (OMAE 2020), American Society of Mechanical Engineers (ASME), 2020.
- [40] P.S. Tromans, L. Vanderschuren, Response based design conditions in the North Sea: application of a new method, in: Proceedings of the Annual Offshore Technology Conference, 1995, pp. 387–397, <https://doi.org/10.4043/7683-ms>. ISBN 9781613990902, ISSN 01603663.
- [41] J. Bowers, I. Morton, G. Mould, Extreme value analysis of the structural response of a single point moored vessel, *Underw. Technol.* 22 (3) (1997) 87–93, <https://doi.org/10.3723/175605497783258986>. ISSN 01410814.
- [42] A. Inceikil, J. Bowers, G. Mould, O. Yilmaz, Response-based extreme value analysis of moored offshore structures due to wave, wind and current, *J. Mar. Sci. Technol.* 3 (1998) 145–150.
- [43] E. Mackay, L. Johanning, A generalised equivalent storm model for long-term statistics of ocean waves, *Coast. Eng.* 140 (2018) 411–428, <https://doi.org/10.1016/j.coastaleng.2018.06.001>.
- [44] E.B.L. Mackay, L. Johanning, A simple and robust method for calculating return periods of ocean waves, in: Proc. 37th International Conference on Ocean, Offshore and Arctic Engineering (OMAE 2018), American Society of Mechanical Engineers (ASME), 2018, <https://doi.org/10.1115/OMAE2018-78729>.
- [45] A.G. Koohi Kheili, Y. Drobyshevski, M. Kimiaeii, M. Efthymiou, Iterative methodology for response based analysis of an FPSO mooring system, *Mar. Struct.* 78 (2021) 102973, <https://doi.org/10.1016/j.marstruc.2021.102973>.
- [46] A.B. Huseby, E. Vanem, B. Natvig, A new approach to environmental contours for ocean engineering applications based on direct Monte Carlo simulations, *Ocean Eng.* 60 (2013) 124–135, <https://doi.org/10.1016/j.oceaneng.2012.12.034>.
- [47] Q. Derbanne, G. de Hauteclercque, A new approach for environmental contour and multivariate de-clustering, in: Proc. 38th International Conference on Ocean, Offshore and Arctic Engineering, OMAE 2019, 2019.
- [48] A.F. Haselsteiner, J.-H. Ohlendorf, W. Wosniok, K.-D. Thoben, Deriving environmental contours from highest density regions, *Coast. Eng.* 123 (2017) 42–51, <https://doi.org/10.1016/j.coastaleng.2017.03.002>.
- [49] W. Chai, B.J. Leira, Environmental contours based on inverse SORM, *Mar. Struct.* 60 (2018) 34–51, <https://doi.org/10.1016/j.marstruc.2018.03.007>.
- [50] P. Agarwal, L. Manuel, Simulation of offshore wind turbine response for long-term extreme load prediction, *Eng. Struct.* 31 (10) (2009) 2236–2246, <https://doi.org/10.1016/j.engstruct.2009.04.002>.
- [51] Q. Li, Z. Gao, T. Moan, Modified environmental contour method to determine the long-term extreme responses of a semi-submersible wind turbine, *Ocean Eng.* 142 (2017) 563–576, <https://doi.org/10.1016/j.oceaneng.2017.07.038>.
- [52] J. Liu, E. Thomas, A. Goyal, L. Manuel, Design loads for a large wind turbine supported by a semi-submersible floating platform, *Renew. Energy* 138 (2019) 923–936, <https://doi.org/10.1016/j.renene.2019.02.011>.
- [53] X. Chen, Z. Jiang, Q. Li, Y. Li, N. Ren, Extended environmental contour methods for long-term extreme response analysis of offshore wind turbines, *J. Offshore Mech. Arctic Eng.* 142 (5), doi: 10.1115/1.4046772 ..
- [54] E.E. Bachynski, M. Collu, Offshore support structure design, in: Renewable Energy from the Oceans: from Wave, Tidal and Gradient Systems to Offshore Wind and Solar, 2019, pp. 271–319, <https://doi.org/10.1049/pbp0129e/TNQDotTNQ/ch7>.
- [55] International Electrotechnical Commission, *Wind Energy Generation Systems - Part 1: Design Requirements*, 2019. Tech. Rep. IEC 61400-1:2019-02.
- [56] A.F. Haselsteiner, R.G. Coe, L. Manuel, W. Chai, B. Leira, G. Clarindo, C. Guedes Soares, N. Dimitrov, A. Sander, J.-H. Ohlendorf, K.-D. Thoben, G. Haute-de, E. Mackay, P. Jonathan, C. Qiao, A. Myers, A. Rode, A. Hildebrandt, B. Schmidt, E. Vanem, A benchmarking exercise for environmental contours, *Ocean Engineering* 236 (2021). <https://doi.org/10.1016/j.oceaneng.2021.109504>.
- [57] G. de Hauteclercque, E. Mackay, E. Vanem, Quantitative Assessment of Environmental Contour Approaches (Preprint from March 2021) (March), doi: 10.13140/RG.2.2.10068.12161 ..
- [58] P. Jonathan, K. Evans, J. Flynn, On the estimation of ocean engineering design contours, *J. Offshore Mech. Arctic Eng.* 136 (4) (2014), <https://doi.org/10.1115/1.4027645>, 41101–1 to 041101–8.
- [59] E. Vanem, E.M. Bitner-Gregersen, Alternative environmental contours for marine structural design – a comparison study, *J. Offshore Mech. Arctic Eng.* 137 (2015), <https://doi.org/10.1115/1.4031063>, 51601–1 to 51601–8.
- [60] A. F. Haselsteiner, E. Mackay, K.-D. Thoben, Reducing Conservatism in Highest Density Environmental Contours (Preprint from January 2021) doi: 10.13140/RG.2.2.35981.56801 ..
- [61] G.S. Baarholm, S. Haver, O.D. Økland, Combining contours of significant wave height and peak period with platform response distributions for predicting design response, *Mar. Struct.* 23 (2) (2010) 147–163, <https://doi.org/10.1016/j.marstruc.2010.03.001>. ISSN 09518339.
- [62] S.R. Winterstein, *Reliability-based prediction of design loads and responses for floating ocean structures*, in: OMAE 1998: 17th International Conference on Offshore Mechanics and Arctic Engineering, 1998.
- [63] Q. Derbanne, G. de Hauteclercque, M. Dumont, How to account for short-term and long-term variability in the prediction of the 100 years response?, in: Proc. 36th International Conference on Ocean, Offshore and Arctic Engineering (OMAE 2017) American Society of Mechanical Engineers (ASME), 2017 <https://doi.org/10.1115/omae2017-61701>.
- [64] E. Vanem, 3-dimensional environmental contours based on a direct sampling method for structural reliability analysis of ships and offshore structures, *Ships Offshore Struct.* 14 (1), doi: 10.1080/17445302.2018.1478377 ..
- [65] J. Jonkman, S. Butterfield, W. Musial, G. Scott, Definition of a 5-MW Reference Wind Turbine for Offshore System Development, Tech. Rep., 2009 <https://doi.org/10.2127/947422>.
- [66] G. Fischer, Installation and operation of the research platform FINO 1 in the North Sea, in: Offshore Wind Energy: Research on Environmental Impacts, Springer, Berlin, Germany, 2006, [https://doi.org/10.1007/978-3-540-34677-7\\_15](https://doi.org/10.1007/978-3-540-34677-7_15). ISBN 3540346767, 237–253.
- [67] N. Groll, R. Weisse, coastDat-2 North Sea Wave Hindcast for the Period 1949–2014 Performed with the Wave Model WAM, 2016, [https://doi.org/10.1594/Wdcc/coastDat-2\\_WAM-North\\_Sea](https://doi.org/10.1594/Wdcc/coastDat-2_WAM-North_Sea).
- [68] N. Groll, R. Weisse, A multi-decadal wind-wave hindcast for the North Sea 1949 – 2014: coastDat-2, *Earth Syst. Sci. Data* 9 (2017) 955–968, <https://doi.org/10.5194/essd-9-955-2017>.
- [69] E. Bachynski, M. Thys, V. Delhay, Dynamic response of a monopile wind turbine in waves: experimental uncertainty analysis for validation of numerical tools, *Appl. Ocean Res.* 89 (2019) 96–114, <https://doi.org/10.1016/j.apor.2019.05.002>.
- [70] National Renewable Energy Laboratory, OpenFAST Documentation: Release 1.0, Tech. Rep, 2010. URL, [https://readthedocs.org/projects/openfast-wave-stretching/downloads/pdf/f-wave\\_stretching/](https://readthedocs.org/projects/openfast-wave-stretching/downloads/pdf/f-wave_stretching/).
- [71] P.J. Moriarty, A. Hansen, AeroDyn Theory Manual, Tech. Rep., National Renewable Energy Laboratory, 2005.
- [72] R. Damiani, J. Jonkman, G. Hayman, SubDyn User 'S Guide and Theory Manual, Tech. Rep., National Renewable Energy Laboratory, 2015.

- [73] S.R. Winterstein, Nonlinear vibration models for extremes and fatigue, *J. Eng. Mech.* 114 (10) (1988) 1772–1790, [https://doi.org/10.1061/\(asce\)0733-9399\(1988\)114:10\(1772\)](https://doi.org/10.1061/(asce)0733-9399(1988)114:10(1772)).
- [74] P. Ragan, L. Manuel, Statistical extrapolation methods for estimating wind turbine extreme loads, *J. Sol. Energy Eng.* 130 (3) (2008), <https://doi.org/10.1115/1.2931501>, 031011–1 to 15.
- [75] A. Naess, O. Gaidai, Monte Carlo methods for estimating the extreme response of dynamical systems, *J. Eng. Mech.* 134 (8) (2008) 628–636, [https://doi.org/10.1061/\(asce\)0733-9399\(2008\)134:8\(628\)](https://doi.org/10.1061/(asce)0733-9399(2008)134:8(628)). ISSN 0733-9399.
- [76] A. Naess, O. Gaidai, Estimation of extreme values from sampled time series, *Struct. Saf.* 31 (4) (2009) 325–334, <https://doi.org/10.1016/j.strusafe.2008.06.021>.